



---

## **Spinneret spinning field ontogeny and life history observations in the spider *Palpimanus uncatus* Kulczyński, 1909 (Araneae: Palpimanidae)**

Author: Townley, Mark A.

Source: The Journal of Arachnology, 52(1) : 41-70

Published By: American Arachnological Society

URL: <https://doi.org/10.1636/JoA-S-22-056>

## Spinneret spinning field ontogeny and life history observations in the spider *Palpimanus uncatus* Kulczyński, 1909 (Araneae: Palpimanidae)

**Mark A. Townley:** University Instrumentation Center, University of New Hampshire, Parsons Hall W123, 23 Academic Way, Durham, New Hampshire 03824, USA; E-mail: mark.townley@unh.edu

**Abstract.** As in other Palpimanidae, two pairs of posterior spinnerets present in typical Araneomorphae are vestigial in *Palpimanus uncatus* Kulczyński, 1909, with only the anterior lateral spinneret (ALS) pair prominent. Nevertheless, in late juvenile and adult females, spigots appear in the ancestral posterior spinneret region (PS). Consistent with these spigots serving cylindrical silk glands, females construct substantial egg sacs. While juveniles and adults exhibit a compressed PS, in postembryos it is fully extended. Piriform silk gland (PI) spigots form a linear array on ALSs from the 1<sup>st</sup> stadium, increasing in number during ontogeny by addition of PIs of the tartipore-accommodated (T-A) subtype (i.e., functional during proecdyses). The number of T-A PIs added from one stadium to the next and locations occupied by their spigots often exhibit a stereotypic pattern, especially consistent in early instars. The number of non-T-A PIs remains constant through ontogeny from the 1<sup>st</sup> stadium: one per ALS rather than the two per ALS inferred in a few araneoids. The secondary major ampullate silk gland (2<sup>o</sup> MaA) spigot, primitively uni-shafted among araneomorphs, has become modified into a multi-shafted spigot with extended base, the number of shafts increasing during ontogeny. However, the multiple ducts that connect to the shafts continue to be accommodated during proecdysis by a single enormous tartipore. Sexual dimorphism is present, with late stadium females having greater numbers of T-A PI spigots and 2<sup>o</sup> MaA spigot shafts. Observations are presented pertaining to feeding behavior, sexual cannibalism (absent), habitat, winter diapause, numbers of molts, and longevity.

**Keywords:** development, molting, Palpimaninae, Palpimanoidea, spinning apparatus  
<https://doi.org/10.1636/JoA-S-22-056>

Spiders within Araneomorphae have multiple silk glands in the opisthosoma that can be divided into different types based on various attributes of the glands and of their outlets, the spigots. Differences among gland types may be evident in their morphologies, histochemistries, locations, fine structures, secretory products (including the number and relative size of distinct secretory cell regions), functions, ontogenetic changes in number, occurrence in one or both sexes (Kovoor 1977, 1987), and gene expression patterns (Clarke et al. 2017). Established silk gland types include epiandrous, cribellar, piriform, major ampullate, aciniform, paracribellar, minor ampullate, cylindrical (= tubuliform), aggregate, and potentially homologous flagelliform/pseudoflagelliform/posterior lateral spinneret (PLS) ‘modified’ silk glands (Griswold et al. 2005; Blackledge et al. 2011; Ramírez 2014; Murphy & Roberts 2015). All but epiandrous silk glands have spigots on the spinnerets. No single species, or family, has all types. See Blackledge et al. (2011) for a review, and Ramírez (2014: table 5) for a tabular summary, of the functions of the different types. Relevant to this study, I note only that, typically, major ampullate silk glands (MaAs) produce draglines and contribute non-sticky silk fibers to webs, piriform silk glands (PIs) produce attachment discs (silk anchors, Wolff et al. 2021) that secure silk fibers, including those of MaAs, to substrates or other fibers, and cylindrical silk glands (CYs) contribute silk fibers to egg sacs.

In some instances, silk glands of one basic type may exist in two or more distinct forms or subtypes within an individual. These may be distinguished from one another based on criteria such as histochemical or morphological characteristics, including morphology of their spigots. Different subtypes are either known or presumed to fulfill different functions or confer different properties within silk constructions. Some Theridiidae, for example, make effective use of two subtypes of aggregate silk gland (AG), one that contributes to the formation of gumfoot lines in webs and the other used directly against prey or predators (Kovoor 1987; Townley & Tillinghast 2013; Clarke et al. 2017; Chaw & Hayashi 2018; Ayoub et al. 2021). Two aciniform silk gland (AC) subtypes, designated A/B or

I/II, are also well-documented in multiple genera of Araneidae (Mullen 1969; Kovoor 1972; Kovoor & Zylberberg 1974; Kovoor & Lopez 1980, 1982, 1988; Lopez et al. 1986; Moon & Kim 1990; Sonavane et al. 2023), and in *Hersilia* Audouin, 1826 (Hersiliidae) (Kovoor 1984), *Polonecia* Lehtinen, 1967 (Uloboridae) (Kovoor & Peters 1988; Peters & Kovoor 1989), and *Nurscia* Simon, 1874 (Titanocidae) (Park & Moon 2009), and this is expanded to three subtypes in *Eriophora* Simon, 1864 (Araneidae) (Kovoor & Peters 1988). Spigot morphology differences indicate additional examples of AC subtypes among a variety of araneomorphs (Griswold et al. 2005; Ramírez 2014). Two subtypes of PI are also known, as in some cyrtophorine Araneidae (Kovoor & Lopez 1982, 1988), Tetragnathidae (Kovoor 1990), and male Clubionidae (Wąsowska 1969; Wiśniewski 1986; Ramírez 2014; Murphy & Roberts 2015); and PI spigot morphologies and arrangements suggest further such examples in some male Liocranidae (Ramírez 2014; Murphy & Roberts 2015) and Mimetidae (Townley & Tillinghast 2009; Townley et al. 2013; Benavides & Hormiga 2016).

Studies involving ampullate silk glands routinely specify either a major ampullate silk gland (MaA) or a minor ampullate silk gland (MiA) identity, and these are often treated as separate silk gland types (as in the first paragraph). They can, however, also be viewed as representing a single type (ampullate) if they are virtually indistinguishable or two subtypes if they differ from one another, e.g., histochemically and morphologically (Kovoor 1977, 1987). In contrast to spigots of AG, PI, and AC subtypes, spigots of MaAs and MiAs are located on separate spinnerets that are derived embryonically from limb buds on different opisthosomal segments (OSSs): MaA spigots on the anterior lateral spinnerets (ALSs), OS4; MiA spigots on the posterior median spinnerets (PMSs), OS5 (Hilbrant & Damen 2015). Thus, an ALS/OS4 or PMS/OS5 association is conveniently specified by identifying ampullate silk glands as MaAs or MiAs, respectively, even in taxa where there is little or no distinction between them other than spigot location (Kovoor 1977, 1987; Řezáč et al. 2017), where any internal distinctions are unknown, or, as in the subject

of this report, where there are no PMS-associated ampullate silk glands.

Silk glands of the same type can also be subdivided based on another criterion: their response to the molt-intermolt cycle (Townley et al. 1993; Tillinghast & Townley 1994; but see Townley & Harms 2017 for terminology as currently applied). In juveniles, as ecdysis approaches (that is, as proecdysis proceeds) and a new exoskeleton forms beneath the old one, the ducts of some silk glands can remain connected to spigots on the old exoskeleton if openings, known as tartipores, form within the developing new exoskeleton around those ducts. These silk glands may be described as tartipore-accommodated (T-A) and silk can potentially be drawn from them throughout proecdysis. The ducts of other silk glands are not accommodated in this way (non-T-A) and become detached from their spigots on the old exoskeleton around the outset of proecdysis (apolysis). Consequently, non-T-A silk glands are unusable during proecdysis. The flip side of this coin, however, is that non-T-A silk glands, once formed, can be used in every subsequent stadium because they are re-modeled during proecdysis (Townley et al. 1991, 1993) and this includes having their ducts re-connect to spigots before ecdysis occurs, but now to spigots on the developing new exoskeleton. In contrast, T-A silk glands, once formed, can only be used in every other stadium because their spigots are shed at ecdysis along with the rest of the old exoskeleton and their ducts do not have the opportunity to re-connect to spigots until the following proecdysis. To have T-A silk glands available in each stadium, therefore, requires two sets of T-A silk glands; one set used in odd-numbered stadia, the other used in even-numbered stadia.

The current study follows from earlier observations on the occurrence of T-A and non-T-A PIs through the ontogenies of several entelegyne spiders. Like other silk gland types that occur as “. . . morphological ‘multiples’ . . . not individually specifiable. . .” (Coddington 1989:81), PIs typically increase in number over an araneomorph spider’s ontogeny (Townley & Harms 2017; Alfaro et al. 2018a; references therein), dramatically in some spiders. Frequently, there is also intraspecific variability in PI number at a given stadium that commonly extends to right/left ALS asymmetry within an individual. In *Araneus* Clerck, 1757 and *Mimetus* Hentz, 1832, type genera of two families within Araneoidea (Wheeler et al. 2017), we found that ontogenetic increases and variability in PI number are entirely due to the development of additional T-A PIs: the number of non-T-A PIs remains constant at two per ALS from the 1<sup>st</sup> stadium to the adult stadium (Townley & Tillinghast 2009). The same pattern occurs in another araneid, *Argiope aurantia* Lucas, 1833 (see Fig. 9e), and in two *Leucauge* White, 1841 species, *L. argyra* (Walckenaer, 1841) and *L. argyrobapta* (White, 1841) (Townley unpublished data), members of the araneoid family Tetragnathidae. PI spigot and tartipore data from two other species of Araneidae, in *Larinioides* Caporiacco, 1934 and *Neoscona* Simon, 1864, are consistent with this pattern (Yu & Coddington 1990). In contrast, all PIs in the Lycosidae examined to date are T-A (Dolejš et al. 2014; isolated observation in Townley & Tillinghast 2009:376) while, conversely, all PIs in the clade composed of Hypochilidae, Filistatidae, and Synspermiata (Wheeler et al. 2017) are non-T-A. Indeed, tartipores are not known to occur at all in this clade (Ramírez 2014). I began this study to determine if the ontogenetically stable character of two non-T-A PIs per ALS occurs outside Araneoidea among more basal taxa within the CY Spigot clade (Wheeler et al. 2017). I selected a species from the type genus of Palpimanidae and Palpimanoidea, *Palpimanus uncatius* Kulczyński, 1909, as the first subject for making this determination, which relied on obtaining spinning field data from

two or more successive exoskeletons from the same individual, a strategy employed previously (Townley & Tillinghast 2009; Dolejš et al. 2014; Townley & Harms 2017). In the course of making observations on PI spigots and tartipores, I documented other spinneret features in *P. uncatius* and these are also presented here.

Palpimanidae are known for their specialized diet (stenophagy) consisting primarily of other spiders (araneophagy) (Pekár et al. 2011a, b, 2022; Pekár & Líznavá 2023) (Fig. 2c) and, related to this feeding preference, for the burly, scopulate first pair of legs present in most species (Fig. 2a,c,d) that are typically held elevated, used for sensing, defense (Fig. 2d), and securing prey rather than for walking (Dippenaar-Schoeman & Jocqué 1997; Cerveira & Jackson 2005; Penney 2009; Le Peru 2011; Pekár et al. 2011b; Logunov et al. 2012; Platnick 2020). A venom that is especially potent against spider prey (Pekár et al. 2018; Michálek et al. 2019) and a thick exoskeleton (Pekár et al. 2011b; Michálek et al. 2017) further enable this ‘stenophagous specialist’ diet (Pekár et al. 2017). Palpimanids are also known for having only a single, well-developed pair of spinnerets, the ALSs (Simon 1892–93; Machado 1944). The PMSs and PLSs are essentially absent, though, in females, they are still represented by spigots of a single type that emerge in the location (compressed along the anterior-posterior axis) where these spinnerets occurred ancestrally (Fig. 5b,d). The family, which extends at least as far back as the early Cretaceous (115–120 Ma) (Downen & Selden 2021), is currently divided into three subfamilies, Palpimaninae, Chediminae, and Otiiothopinae (Platnick 1975; Wheeler et al. 2017), made up of 3, 14, and 4 genera and 45, 49, and 78 species, respectively (Platnick 1981; Platnick et al. 1999; Zonstein & Marusik 2013, 2017, 2022; Lin & Li 2020; Oketch et al. 2020; World Spider Catalog 2024).

Spinnerets of palpimanids have been closely examined in earlier studies. Those of *Palpimanus gibbulus* Dufour, 1820, a member of Palpimaninae, have been described, and detailed drawings presented, in both Machado (1944) and Murphy & Roberts (2015). The former study, based on examination of juvenile and adult females, did not delve into specific silk gland types, but provided the rationale for (correctly) identifying the single pair of spinnerets as ALSs, as opposed to a presumption by Petrunkevitch (1933, 1942) of a PLS identity. In Murphy & Roberts (2015), the spigots of female and male adults were identified by silk gland type, including identifying the female-specific spigots located between the ALSs and anal tubercle as CY spigots. The silk gland types they identified agree with those in this report. They also provided spinneret drawings of male and female specimens of *Boagrius pumilus* Simon, 1893, a representative of Chediminae. Significantly, the drawings show a clear difference between *Palpimanus* Dufour, 1820 and *Boagrius* Simon, 1893 with respect to MaA spigots, those of *Boagrius* mostly typical for a CY Spigot clade spider (2/ALS, though with a nubbin also indicated) while those of *Palpimanus* are decidedly unusual, garnering the designation ‘modified major ampullate gland spigots’ from Murphy & Roberts (2015) for certain of these spigots. Nevertheless, observations presented here indicate that the MaA spigots of *P. uncatius* are readily homologized with non-T-A [primary (1°)] and T-A [secondary (2°)] MaA spigots (see Terminology) present in other members of the CY Spigot clade. From the Otiiothopinae, Platnick et al. (1991) examined by scanning electron microscopy (SEM) the spinnerets of adult female and male specimens of *Otiiothops pentucus* Chickering, 1968. They noted similarities to *Palpimanus* based on observations in Machado (1944)—PI spigots in a linear array, posterior spinnerets absent but female-specific spigots occupying their

location—with uncertainty expressed about a CY identity for the latter spigots that was again expressed in the descriptions of *Otiiothops atlanticus* Platnick, Grismado & Ramírez, 1999 and the otiiothopine genus *Notiiothops* Platnick, Grismado & Ramírez, 1999 (Platnick et al. 1999). Scans of ALSs from *O. pentucus* in Platnick et al. (1991) are difficult to interpret in terms of MaA spigots, but in their cladistic analysis *Otiiothops* MacLeay, 1839 was coded as having one MaA spigot per ALS. If correct, this would be a departure from the state existing in *Palpimanus* and *Boagrius*.

This study builds on these earlier investigations, providing observations that are germane to the instigating concern (ontogenetic changes in T-A and non-T-A PIs) but also to other aspects of spinning field development, use, and evolution in *Palpimanus*. In addition, I present life history observations for *P. uncatus*, made at the time of specimen collection and in the laboratory, including some particularly relevant to the spinning apparatus (e.g., egg sac construction, post-prey-capture abdomen lifts (Watts & Townley 2022)). Finally, I include images of copulatory structures of *P. uncatus*, both to document the species under consideration here (should species identification be in question, female palpimanids especially presenting a challenge (e.g., Platnick 1975)) and to enlarge the pool of available depictions of these structures. The World Spider Catalog (2024) lists five taxonomic references for *P. uncatus* and these include but a single illustration of female internal genitalia, original to Platnick (1981), adapted in Le Peru (2011).

## TERMINOLOGY

I follow Downes (1987) in naming developmental stages. Consecutively numbered **instars** and **stadia** are applied to spiders and periods of time, respectively, between ecdyses or following the final ecdysis. Hatching of the embryo releases the **postembryo** (Fig. 7a) and ecdysis and discarding of the resulting exuvium by the postembryo produces the **1<sup>st</sup> instar** and initiates the **1<sup>st</sup> stadium**.

**Proecdysis** covers much of the molting sequence, extending from apolysis (separation of the exoskeleton from the underlying epidermis) up to ecdysis (shedding of the old exoskeleton). Among other processes, a new exoskeleton develops under the old exoskeleton during proecdysis. For a spider that is in proecdysis, **pharate** refers to all of the spider from its new exoskeleton inward (i.e., excluding its old exoskeleton). Thus, I use pharate in this report, and **Ph** in figures, to identify spinnerets and spinning structures on a developing, new exoskeleton that were still concealed beneath the old exoskeleton at the time of the spider's death. For example, the label '4<sup>th</sup> (Ph)' used in Fig. 8d signifies that the image shows part of a pharate 4<sup>th</sup> instar's newly formed exoskeleton (an ALS spinning field in this example) as it existed during proecdysis within a spider that, overall, I consider to still be a 3<sup>rd</sup> instar (see Townley & Harms 2017: fig. 1). The old exoskeleton of this 3<sup>rd</sup> instar is shown in Fig. 8c.

The openings (short conduits or collared pores) called **tartipores** that function during proecdysis are explained in the introductory comments, as are **T-A** and **non-T-A** silk glands. Examples of tartipores that were clearly still in use in the pharate exoskeletons of proecdysial spiders may be seen in Figs. 10d–f and 13c. Their functionality is demonstrated by the silk gland ducts that they encircle. These ducts connected to spigots on the old exoskeleton and became detached from them during spinneret preparation for SEM (see Methods). The usefulness of tartipores in the newly formed exoskeleton ends at ecdysis with the shedding of the old exoskeleton and its

spigots, but the tartipores remain visible in the exoskeleton subsequently as cuticular scars. Post-functional tartipores may be seen in multiple figures, especially well (and un-colored) in the exuvium shown in Fig. 13a,b. Each individual T-A silk gland functions during either odd-numbered stadia or even-numbered stadia. To specify the group of T-A silk glands functioning during odd-numbered stadia, or a subset of these distinguished by (sub)type, I refer to them as an **odd-stadia set** of T-A silk glands. Likewise, an **even-stadia set** of T-A silk glands can be specified.

As extensive published SEM scans indicate (Griswold et al. 2005; Ramírez 2014; Ramírez et al. 2014), the MaAs of many spiders within the CY Spigot clade can be divided into T-A and non-T-A MaAs. These have been referred to as **secondary (2°)** and **primary (1°) MaAs**, respectively, to emphasize differences in size and extent of use that exist in some taxa (Townley et al. 1993; Řezáč et al. 2017; references therein). I use those designations here for consistency and to stress homologies proposed between 1° and 2° MaAs of *P. uncatus* and other CY Spigot clade araneomorphs.

A silk gland spigot typically consists of a proximal **base** and more distal **shaft**. The most distal (apical) part of a spigot's shaft, containing the opening through which a silk fiber is drawn, may be distinct from the rest of the shaft and has been termed the **endpiece** (Kovoor & Peters 1988). Spigots are typically **uni-shafted**, one shaft on one base. But some are **multi-shafted**, with multiple shafts sharing a common base. In *P. uncatus*, the spigots serving 2° MaAs are multi-shafted. Each shaft on a shared base has its own duct which is, in turn, likely connected to a separate silk gland. It is therefore legitimate to refer to a multi-shafted spigot (singular), alternatively, as spigots (plural) on a common base. But in this report I use the singular when referring to one multi-shafted spigot, both to emphasize the 2° MaA spigot homology proposed between *P. uncatus* and other CY Spigot clade members and because a multi-shafted spigot forms a single entity when considered in its entirety. On the other hand, the ducts and silk glands served by one multi-shafted spigot, and the shafts on such a spigot, I refer to in the plural. Thus, one multi-shafted spigot serves multiple silk glands.

## ABBREVIATIONS USED IN TEXT AND FIGURES

1°	primary
2°	secondary
AC/s	aciniform silk gland/s
AG/s	aggregate silk gland/s
ALS/s	anterior lateral spinneret/s
CLSM	confocal laser scanning microscop(e)y
CY/s	cylindrical (= tubuliform) silk gland/s
MaA/s	major ampullate silk gland/s
MiA/s	minor ampullate silk gland/s
MS	PLS modified silk gland [possible homolog of flagelliform and pseudoflagelliform silk glands]
non-T-A	non-tartipore-accommodated
OS/s	opisthosomal segment/s
PC	paracribellar silk gland
PI/s	piriform silk gland/s
PLS/s	posterior lateral spinneret/s
PMS/s	posterior median spinneret/s
PS/s	posterior spinneret region/s [ancestrally occupied by PMSs + PLSs]
RL	reflected light
SDS	sodium dodecyl sulfate
SEM	scanning electron microscop(e)y
T-A	tartipore-accommodated
TL	transmitted light



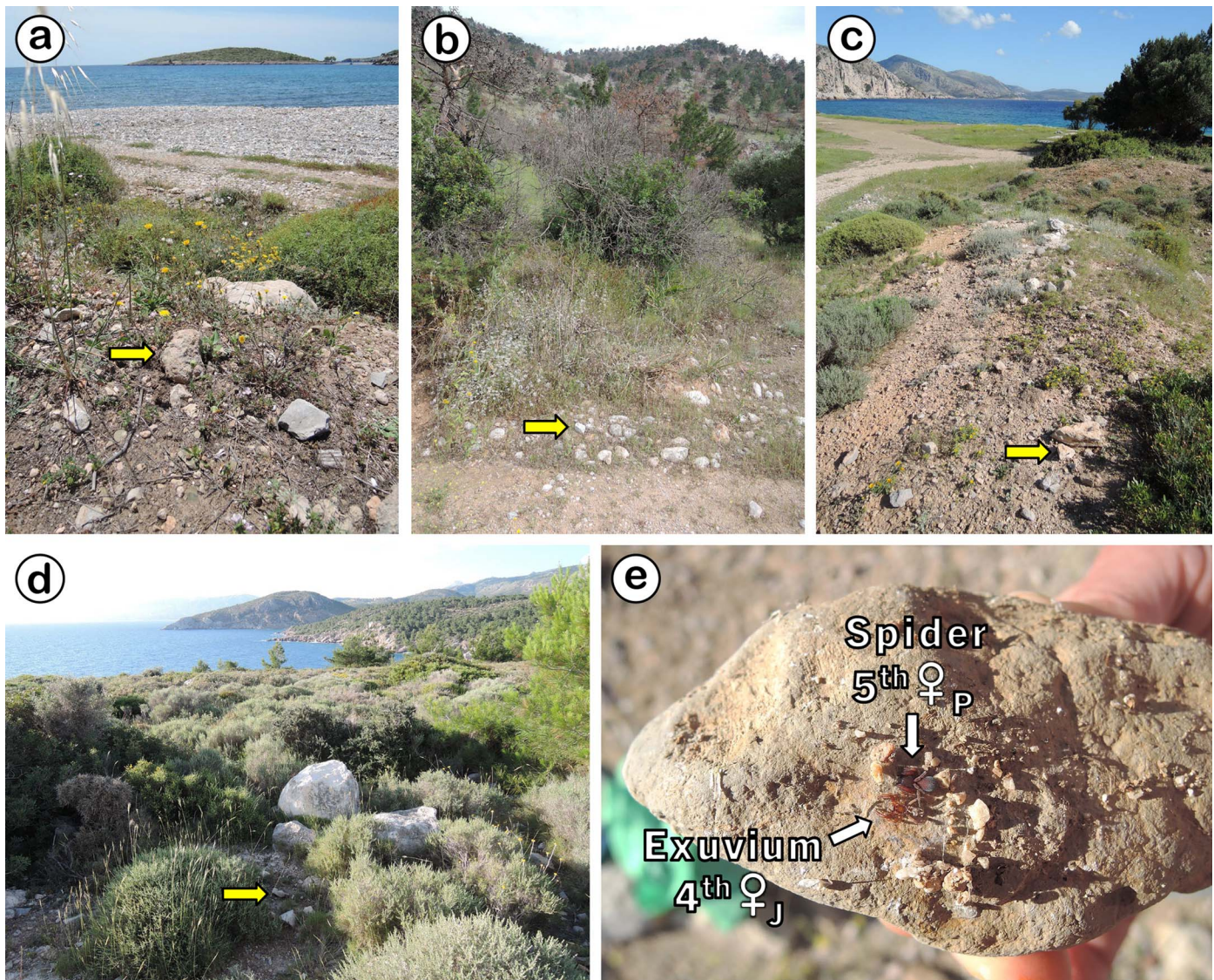


Figure 1.—Example habitat of *Palpimanus uncatus* on Chios (Greece). (a) Close to Aggelia Beach, 38°13'23"N, 25°54'24"E, elevation 17 m. (b) Inland (0.3 km) from Elinda Beach, 38°23'36"N, 25°59'37"E, elevation 6 m. (c) Inland (0.09 km) from Makria Ammos Beach, 38°24'09"N, 25°58'13"E, elevation 6 m. (d) Cape Pirghos, 0.2 km from coast, 38°24'16"N, 25°57'44"E, elevation 40 m. (e) Specimen UNHC\_0049460 of *P. uncatus* at Cape Pirghos found on underside of rock by CD Newton, photographed right after rock picked up; spider side by side with most recently shed exuvium. Note pebbles/sand grains that had apparently been incorporated into the spider's silk retreat on underside of rock. Yellow arrows (a–d) point to individual rocks from beneath which specimens of *P. uncatus* UNHC\_0049458, UNHC\_0049457, UNHC\_0049453, and MCZ\_IZ\_163565, respectively, were collected.

## METHODS

**Spider collection.**—From 10–18 May 2014, CD Newton, LM Newton, and I collected 23 live specimens of *Palpimanus uncatus* (but see comments on species identity in Results) on the island of Chios (Χίος, Khíos), Greece (38°23'N, 26°03'E; see Supplemental Appendix 1 for detailed location data, online at <https://doi.org/10.1636/JoA-S-22-056.s1>) by searching under rocks on public land (Permit no. 104696/161 issued by the Ministry of the Environment of Greece) (Fig. 1). These included one juvenile, sex unknown (3<sup>rd</sup> instar); seven female juveniles (4<sup>th</sup>–6<sup>th</sup> instars) plus adjacent exuvia for two of these; nine male juveniles (3<sup>rd</sup>–4<sup>th</sup> instars) plus an adjacent exuvium for one of these; five female adults (6<sup>th</sup> instars), one carrying an egg sac; and one male adult (6<sup>th</sup> instar). In addition, we collected

two exuvia of 3<sup>rd</sup> instars (sex unknown) and one exuvium of a female 4<sup>th</sup> instar without the spiders that shed them. While still on Chios, one male 4<sup>th</sup> instar (UNHC\_0049457) died a week after capture, possibly bitten by an introduced spider intended as prey.

**Spider maintenance, rearing, and storage.**—We transported spiders to the University of New Hampshire on 22 May 2014 where I set up the 22 remaining live *P. uncatus* individually in wood boxes with flip-top screened lids (outside: 13.5 x 7.5 x 8 cm; inside: 12 x 6.2 x 6.5 cm), containing a layer of sandy soil about 1 cm deep. I initially placed one or two rocks in each box under which spiders hid. But because the focus of this study is spinneret spinning fields, it was desirable to get exuvia and any spiders that died immersed in detergent solution and 75% ethanol, respectively, as soon as possible. Thus, I inspected box interiors and



rock undersides on most days. These regular disturbances, with accompanying damage to silk retreats embedded with sand grains (Fig. 1e), presumably made residence under rocks less appealing and spiders were increasingly found elsewhere within the box. I therefore removed rocks after about 2–4 weeks depending on the spider.

Through the remainder of spring, summer, and into autumn 2014, I kept boxes in a partially shaded greenhouse, with a large window running its length left open so that temperature, humidity, and light conditions mirrored those of southeast New Hampshire. With decreasing daylight hours and temperature in the autumn (and again in autumn 2015) spiders seemed to enter a period of diapause. I closed the greenhouse window and set a thermostat so the temperature did not fall below about 8°C, a typical monthly average minimum temperature spiders experience on Chios in winter (World Weather Online 2022). In spring 2015, spiders emerged from diapause and I re-opened the window.

*P. uncatus* preyed upon a variety of juvenile and adult field-collected spiders (see Results for families to which prey spiders belonged). I generally added a single live prey spider to a box during a feeding attempt, but occasionally two were added if both were considerably smaller than the *P. uncatus*. If a spider was not preyed upon within two days, I offered it to another individual. I did not impose a specific feeding regimen but 17 of the 22 *P. uncatus* captured and fed on a spider (or two smaller spiders) during each of 9 to 27 feedings ( $\bar{X} \pm SD = 19 \pm 5.5$  feedings) while in captivity (see Results for frequency of successful feeding). I sprayed a mist of water directly on spiders almost daily (weekly during diapause).

I stored exuvia that were collected in the field and those shed in the greenhouse in 2X-strength Novex™ Tris-glycine sodium-dodecyl-sulfate (SDS) buffer (ThermoFisher Scientific, LC2675) at room temperature to help render them pliable and clean.

Three female and four male spiders collected as juveniles reached adulthood in the greenhouse and by April 2015 seven female and five male adults were available to attempt matings, in the hope that these would result in viable egg sacs. Between 20 April and 26 August 2015, I housed each male with each female (with two exceptions) for an arbitrary period of 4–73 days.

I maintained spiders in the greenhouse until they died (15 spiders) or until I euthanized (CO<sub>2</sub>) and stored them in 75% ethanol on 21 November 2015 (7 spiders). I terminated the latter group, consisting of adults (3 ♀, 4 ♂), because by this date a few individuals were exhibiting spinneret fouling by fecal material and I decided to preserve all but two of the remaining live specimens before further fouling occurred.

The two spiders that were maintained beyond 21 November 2015 were female, already mature when field-collected, and each produced one viable egg sac in the greenhouse. One female (MCZ\_IZ\_163558) died on 5 February 2016 during her second winter diapause in the greenhouse, the other (UNHC\_0049452) on 30 October 2016 shortly after entering a third winter diapause. Attempts were made to raise a small number of offspring from the two egg sacs, with very limited success. Nevertheless, these attempts did supply specimens at stages (postembryonic, 1<sup>st</sup> and 2<sup>nd</sup> juvenile stadia) not collected in the field. Feeding and watering of the early instars was the same as for later instars except that I kept them in 20 ml glass scintillation vials containing paper towel, water was applied to the towel, and introduced prey spiders were appropriately small.

Voucher specimens are deposited in the Museum of Comparative Zoology at Harvard University (MCZ, IZ\_163556-163566) and in the Collection of Insects and Other Arthropods at the

University of New Hampshire (UNHC, 0049451-0049461, 0049463) (Supplemental Appendix 1). Taxonomy in this paper follows the World Spider Catalog (2024).

**Spinneret preparation for scanning electron microscopy (SEM).**—I prepared spinnerets for SEM using the methods detailed in Townley & Harms (2017). To summarize, from spiders preserved in 75% ethanol, I severed from the opisthosoma, as a unit, the portion containing the tracheal spiracle, spinnerets, and anal tubercle and immersed it for 3 or more days in the buffered SDS solution given above. This was followed by enzyme digestion using a contact lens cleaner. With the preparation submerged in SDS buffer, I then pulled each of the ALSs down onto a blunted pin tip sticking up from a wax substrate to expand them more fully. Dehydration through an ethanol series, critical point drying, mounting, and Au/Pd sputter coating preceded examination on a Tescan Lyra3 GMU field-emission SEM at 6kV.

If a spider was well into proecdysis at the time of death, the old and developing exoskeletons separated from one another during their immersion in the commercial contact lens cleaner. These I continued processing, and then examined by SEM, separately. This occurred six times, two of these being progeny from egg sacs built in the laboratory. I identify spinneret cuticle forming part of the developing exoskeleton as ‘pharate’ (Ph in figures) to distinguish it from spinneret cuticle composing the old exoskeleton.

I processed spinnerets on exuvia, stored in SDS buffer, like spinnerets from the spiders themselves except that I omitted the treatment with contact lens cleaner.

The color coding of spigots and tartipores used on SEM scans in Figs. 7–11 follows the procedure of Dolejš et al. (2014). The key to these colors is given in Fig. 6.

**Species identification and examination of genitalia.**—I examined specimens and dissected females on an Olympus SZX12 stereomicroscope. Descriptions in Kulczyński (1909) and Platnick (1981) were used to identify all adults to species. Transmitted light (TL) microscope images of male palps from two individuals, in Hoyer’s medium on temporary slide mounts (Coddington 1983), were captured on an inverted Nikon Eclipse Ti2 compound microscope with a DS-Ri2 color CMOS camera controlled with NIS-Elements software (version 5.21.03) running the ‘Real Time Extended Depth-of-Focus’ option. This microscope and software are also components of the Nikon A1R HD confocal laser scanning microscope (CLSM) system I refer to below for imaging autofluorescence from female genitalia. Following TL microscopy, the palps from one male were briefly rinsed in distilled water before being processed and examined by SEM as described above for spinnerets, starting at dehydration through an ethanol series.

I dissected internal genitalia of female adults in 75% ethanol using Vannas spring scissors (Fine Science Tools, 15000-08) to separate opisthosomal scutum and adjacent cuticle and structures, including genitalia and book lungs, from the rest of the opisthosoma. Fine forceps and insect pins were then used to expose the internal genitalia. I obtained TL and reflected light (RL) microscope images of genitalia from three individuals on the Olympus SZX12 stereomicroscope using a Zeiss Axiocam 503 color camera controlled by Zeiss ZEN 2 Blue Edition software (version 2.3.69.1000) with manual extended depth-of-focus. TL images were also obtained on the compound microscope as described above for male palps except that 75% ethanol was used as mounting medium since shrinkage of spermathecae was noted with use of Hoyer’s medium or glycerol. With two specimens, multichannel epifluorescence images were

captured as confocal (1.2 Airy unit) Z-stacks on the Nikon AIR HD CLSM, taking advantage of the autofluorescence emitted from unstained genitalia preparations within the ranges 425–475, 500–550, 570–620, and 663–738 nm when excited at 409, 488, 560, and 639 nm, respectively. Z-stacks were processed with the above NIS-Elements Extended Depth-of-Focus software to generate the fluorescence images in Fig. 4d,f,i.

All microscopes used are part of the University of New Hampshire's Instrumentation Center (<https://www.unh.edu/uic>).

**Estimation of stadia.**—I estimated the stadium a spider was in when field-collected based on a combination of carapace dimensions, numbers of PI spigots and tartipores, numbers of 2° MaA shafts, and, for females, numbers of CY spigots. Having one or more exuvia from an individual was helpful in making this estimate. I obtained carapace dimensions from images collected on the calibrated Olympus SZX12 stereomicroscope and numbers of spinning field structures from SEM scans.

RESULTS

**Habitat.**—All *P. uncatus* and their exuvia collected on Chios were found under rocks that were in contact with soil, at sites close to the coastline where we focused our search efforts (Fig. 1a–d; Supplemental Appendix 1). Three juveniles collected (2 ♀, 1 ♂) had an exuvium nearby, attached to the underside of the same rock (Fig. 1e). Data obtained from these exuvia (Tables 1, 2) were entirely consistent with them being the most recent exoskeletons shed by the adjacent spiders and I treat them as such here. Fifteen of the collected spiders were secured to the underside of the rock when found; the other eight were on the soil beneath the rock.

**Egg sacs and attempted matings.**—One female adult (MCZ\_IZ\_163566) was holding an egg sac with her chelicerae when discovered on the underside of a rock on 18 May 2014 (Fig. 2a). Viewed from above, the egg sac was nearly circular with an average diameter of 6.1 mm (Fig. 2b left) and height of 4.4 mm (Fig. 2b right). Its nearly flat bottom was thinner and more translucent than the rest of the egg sac and the top portion tapered shallowly to a point (Fig. 2a,b right). Most often the mother held the egg sac by the point (Fig. 2a), but not exclusively. Forty-four days after being collected, no spiderlings had emerged from the egg sac, so I opened it, finding 38 shriveled whitish to brownish eggs, all unhatched. One additional egg sac was built by this female on 22 July 2014, but after five days it was found mangled and contained no eggs (possibly consumed by mother). Similarly, a second female (not deposited in a collection) collected as an adult made an egg sac on 15 July 2014 but ten days later I found the bottom of the egg sac open and the sac empty.

Two other females collected as adults yielded hatched progeny, their egg sacs produced two days apart. One of these (UNHC\_0049452) made an egg sac on 22 June 2014 and 38 days later, on 30 July, five 1<sup>st</sup> instars emerged from the egg sac and another three 1<sup>st</sup> instars, a postembryo close to ecdysing, and six undeveloped eggs were inside the egg sac. The other female (MCZ\_IZ\_163558) made an egg sac on 20 June 2014, and after 34 days, on 24 July, two 1<sup>st</sup> instars and six postembryos (five dead) were outside the egg sac and six unhatched eggs were inside, though one of the latter had at least largely completed embryonic development. On this day, the mother appeared to be feeding on an undeveloped egg and her mouthparts were near an opening that had been made in the wall of the egg sac. A second egg sac was constructed by this female on 23 August 2014 but nine days later its bottom was partially open, revealing nine shriveled eggs inside. The

Table 1.—Numbers of spinning structures, carapace dimensions, and prevalence of 2° MaA silk fibers on exuvia during the ontogeny of *Palpimanus uncutus*. See Abbreviations section for abbreviations used. Data presented as integers if no variation observed; otherwise, as means ± their standard errors (for ALS-relevant columns, calculated using mean from each ALS pair) and, in parentheses, ranges (for ALS-relevant columns, across all individual ALSs). Standard errors for proportions calculated as in Heath (1995). Numbers of observations *n*<sub>1</sub>, *n*<sub>2</sub>, *n*<sub>3</sub> apply to data columns to their right, up to the next *n*. NA, not applicable; PE, postembryo; PI, postembryo; Penult, penultimate (subadult); TP, tartipore primordium.

Instar	Sex	<i>n</i> <sub>1</sub>	Structures per ALS					Entire PS				Carapace length (mm)	Carapace width (mm)		
			PI spigots	PI tartipores	1° MaA spigots	2° MaA tartipores	2° MaA shafts	CY spigots	<i>n</i> <sub>2</sub>	Proportion of 2° MaA shafts on exuvia bearing silk fibers	<i>n</i> <sub>3</sub>				
PE	?	2	0	0	0	0	0	0	0	0	0	0	—	—	
1 <sup>st</sup>	?	11	2	0	1	1	1	TP	4.2 ± 0.14 (3-5)	0	4	0.35 ± 0.239 (0.00-0.80)	7	0.95 ± 0.010 (0.93-1.00)	0.76 ± 0.014 (0.71-0.82)
2 <sup>nd</sup>	?	6	3	1	1	1	1	1	4.7 ± 0.21 (4-6)	0	0	—	4	1.15 ± 0.031 (1.08-1.20)	0.87 ± 0.017 (0.82-0.89)
3 <sup>rd</sup>	♀ + ♂	7	4	2	1	1	1	1	7.8 ± 0.32 (6-10)	0	4	0.50 ± 0.250 (0.00-0.88)	2	1.56 ± 0.100 (1.46-1.66)	1.18 ± 0.105 (1.07-1.28)
4 <sup>th</sup>	♀	6	4.8 ± 0.11 (4-5)	2.8 ± 0.11 (2-3)	1	1	1	1	9.8 ± 0.34 (8-11)	3.8 ± 0.98 (0-6)	5	0.42 ± 0.221 (0.00-1.00)	4	1.92 ± 0.043 (1.83-2.03)	1.49 ± 0.054 (1.34-1.57)
4 <sup>th</sup>	♂	9	4.9 ± 0.11 (4-5)	3	1	1	1	1	9.2 ± 0.28 (8-11)	0	5	0.53 ± 0.223 (0.00-1.00)	8	1.81 ± 0.056 (1.55-2.03)	1.40 ± 0.045 (1.23-1.62)
5 <sup>th</sup>	♀	6	6.3 ± 0.31 (5-8)	3.8 ± 0.11 (3-4)	1	1	1	1	13.8 ± 0.88 (11-18)	21.0 ± 2.49 (14-31)	3	0.57 ± 0.286 (0.13-1.00)	4	2.28 ± 0.069 (2.11-2.44)	1.81 ± 0.093 (1.71-2.09)
5 <sup>th</sup>	♂	6	5.7 ± 0.25 (4-6)	3.8 ± 0.17 (3-4)	1	1	1	1	11.8 ± 0.46 (10-14)	0	4	0.75 ± 0.217 (0.50-0.93)	4	2.12 ± 0.156 (1.65-2.30)	1.74 ± 0.148 (1.30-1.91)
6 <sup>th</sup> Penult	♀	8	7.0 (6-8)	5	1	1	1	1	16.5 (16-17)	28	0	—	1	2.65	2.05
6 <sup>th</sup> Adult	♀	8	8.6 ± 0.37 (7-11)	5.6 ± 0.36 (4-8)	1	1	1	1	17.7 ± 0.76 (14-23)	36.6 ± 1.29 (33-44)	8	NA	8	2.84 ± 0.066 (2.58-3.08)	2.27 ± 0.048 (2.09-2.49)
6 <sup>th</sup> Adult	♂	5	6.6 ± 0.19 (6-7)	4.9 ± 0.10 (4-5)	1	1	1	1	10.2 ± 0.60 (8-12)	0	5	NA	5	2.70 ± 0.040 (2.63-2.81)	2.16 ± 0.036 (2.07-2.25)
7 <sup>th</sup> Adult (pharate)	♀	1	11.5 (11-12)	6.0 (5-7)	1	1	1	1	21.5 (21-22)	41	0	NA	0	—	—

Table 2.—Numbers of T-A and non-T-A PIs served by PI spigots during the ontogeny of *Palpimanus uncatus*. Determined using consecutive exoskeletons from the same individual by comparing numbers of PI spigots on each ALS of one exoskeleton with numbers of PI tartipores on the corresponding ALSs of the next exoskeleton. See Abbreviations section for abbreviations used. Data presented as integers if no variation observed; otherwise, as means  $\pm$  their standard errors, calculated using mean from each ALS pair, and, in parentheses, ranges across all individual ALSs. Penult, penultimate (subadult).

Instar	Sex	<i>n</i>	PIs per ALS	
			Non-T-A	T-A
1 <sup>st</sup>	♀ + ♂	5	1	1
2 <sup>nd</sup>	♀ + ♂	1	1	2
3 <sup>rd</sup>	♀	1	1	3
3 <sup>rd</sup>	♂	2	1	3
4 <sup>th</sup>	♀	5	1	3.8 $\pm$ 0.12 (3-4)
4 <sup>th</sup>	♂	6	1	3.8 $\pm$ 0.17 (3-4)
5 <sup>th</sup>	♀	3	1	5.3 $\pm$ 0.60 (4-7)
5 <sup>th</sup>	♂	4	1	4.9 $\pm$ 0.13 (4-5)
6 <sup>th</sup> Penult	♀	1	1	6.0 (5-7)

two egg sacs from which 1<sup>st</sup> instars emerged had openings that seemed larger than the 1<sup>st</sup> instars could have created, or needed to emerge, and were presumably made by the mothers. Manipulation by the mother would also explain the largely immotile postembryos found outside one opened egg sac. All egg sacs were white.

Attempts made at mating *P. uncatus* did not result in the formation of any egg sacs; not even non-viable ones. No sexual cannibalism occurred during the sometimes prolonged periods of cohabitation by male-female pairs.

**Prey.**—I made no attempt to feed *P. uncatus* non-spider prey. Field-collected juvenile and adult *P. uncatus* successfully preyed and fed upon spiders from the families Agelenidae, Araneidae, Cheiracanthiidae (Fig. 2c), Dictynidae, Gnaphosidae, Linyphiidae, Lycosidae, Oecobiidae, Philodromidae, Pholcidae, Pisauridae, Salticidae, Tetragnathidae, Theridiidae, Thomisidae, and Uloboridae. 1<sup>st</sup> and 2<sup>nd</sup> instars raised from the two viable egg sacs successfully preyed upon members of Araneidae, Cheiracanthiidae, Salticidae, and Tetragnathidae. Early experiences with feeding *P. uncatus* a range of spiders suggested that salticids were especially likely to be preyed upon quickly, successfully, and their tissues largely consumed. Collecting efforts therefore became aimed at capturing members of this family to feed *P. uncatus*, though not to the exclusion of spiders from other families as encountered.

The mean time between successful feedings, not including periods of winter diapause, was 12.6 days with a high standard deviation of 11.6 days ( $n = 295$ ), in part because of periods when *P. uncatus* were unreceptive to prey (e.g., approaching a molt or egg sac construction). Females tending egg sacs, however, did capture and feed on prey spiders.

Prey capture was directly observed in only a few instances (Fig. 2c). Once a prey spider was immobilized, *P. uncatus* engaged in a series of abdomen lifts on and in the vicinity of the prey (Watts & Townley 2022). These were part of the spider's behavioral repertoire from earliest stadia, noted in one 1<sup>st</sup> instar, one 2<sup>nd</sup> instar, and two female

adults after subduing prey. When abdomen lifts took place on a sandy substrate, sand grains were seen to levitate from the surface as the abdomen was lifted, demonstrating that silk, though not directly visible under the viewing conditions, was being drawn during these lifts. The silk drawn was presumably MaA and/or PI silk given that 1<sup>st</sup> and 2<sup>nd</sup> instars, as well as female adults, performed this behavior. One female adult (MCZ\_IJZ\_163556) performed abdomen lifts for about 30 min after seizing an agelenid, with the first few lifts made while the agelenid was still in her chelicerae. She then set the agelenid down, made lifts directly over it, and then continued making lifts while moving a few centimeters away from the prey. She returned to the prey, contacted it, then set off in another direction. This was repeated four more times, all while performing abdomen lifts, before she settled and began feeding. Speculatively, these applications of silk both on the prey and at some distance from it may help secure the prey as well as alert the *P. uncatus* to approaching intruders. Abdomen lifts were not limited to bouts after prey capture (e.g., also noted when establishing a new retreat), but I observed this extended series of lifts at short intervals only at such times.

On three occasions, *P. uncatus* in the greenhouse fell prey to other spiders (two theridiids, one salticid), a not unusual occurrence, at least when *Palpimanus* and another spider are confined together in the laboratory (Pekár & Líznavá 2023). One of these was not an intended introduction: a female 5<sup>th</sup> instar (UNHC\_0049460) that last accepted prey on 2 August 2015 and that was in winter diapause, was killed by an unidentified juvenile theridiid on 8 November 2015 that happened to be living in the greenhouse and was small enough (before feeding) to penetrate the mesh of the box lid. Another possible victim of winter diapause vulnerability was a 2<sup>nd</sup> instar that last fed on 14 October 2014 and was killed 12 April 2015 by a 1<sup>st</sup> or 2<sup>nd</sup> instar of *Steatoda grossa* (C.L. Koch, 1838). The third occasion was the one instance where a reliance on salticids as prey failed: a female 6<sup>th</sup> instar (MCZ\_IJZ\_163557) was killed by a slightly larger salticid on 12 September 2014. This female was later found to have been well into proecdysis, another potentially vulnerable period. She was the source of the spinning fields shown in Fig. 10c–e.

**Winter diapause.**—Thirteen of the field-collected *P. uncatus* completed the 2014–2015 period of winter diapause in the greenhouse and one female adult (UNHC\_0049452) completed the 2015–2016 winter diapause as well. Diapause in New Hampshire lasted, at a minimum, from late October to mid-March. For the 2014–2015 group of thirteen, the last successful pre-diapause feeding took place between 6 September and 22 October 2014 and the first successful post-diapause feeding occurred between 23 March and 19 April 2015. Whether a comparable period of diapause occurs in the Mediterranean region is not known.

**Molts to maturity and longevity.**—The five male adults and eight female adults obtained during this study are estimated to have been in the 6<sup>th</sup> stadium and thus molted six times before reaching maturity (Table 1). One female penultimate instar that was in proecdysis when she was killed by a salticid (see 'Prey' above) is estimated to have been a 6<sup>th</sup> instar that would have been a 7<sup>th</sup> stadium adult. This possible variability among females, however, needs to be confirmed as uncertainty estimating stadia was most pronounced among such late instar females.

Regarding potential longevity, one female (UNHC\_0049452) was already a mated adult when collected on 18 May 2014, producing a viable egg sac about a month later. She died more than 29 months after collection on 30 October 2016, so was presumably at least 3 years old when she died. For males, a potential lifespan of at least



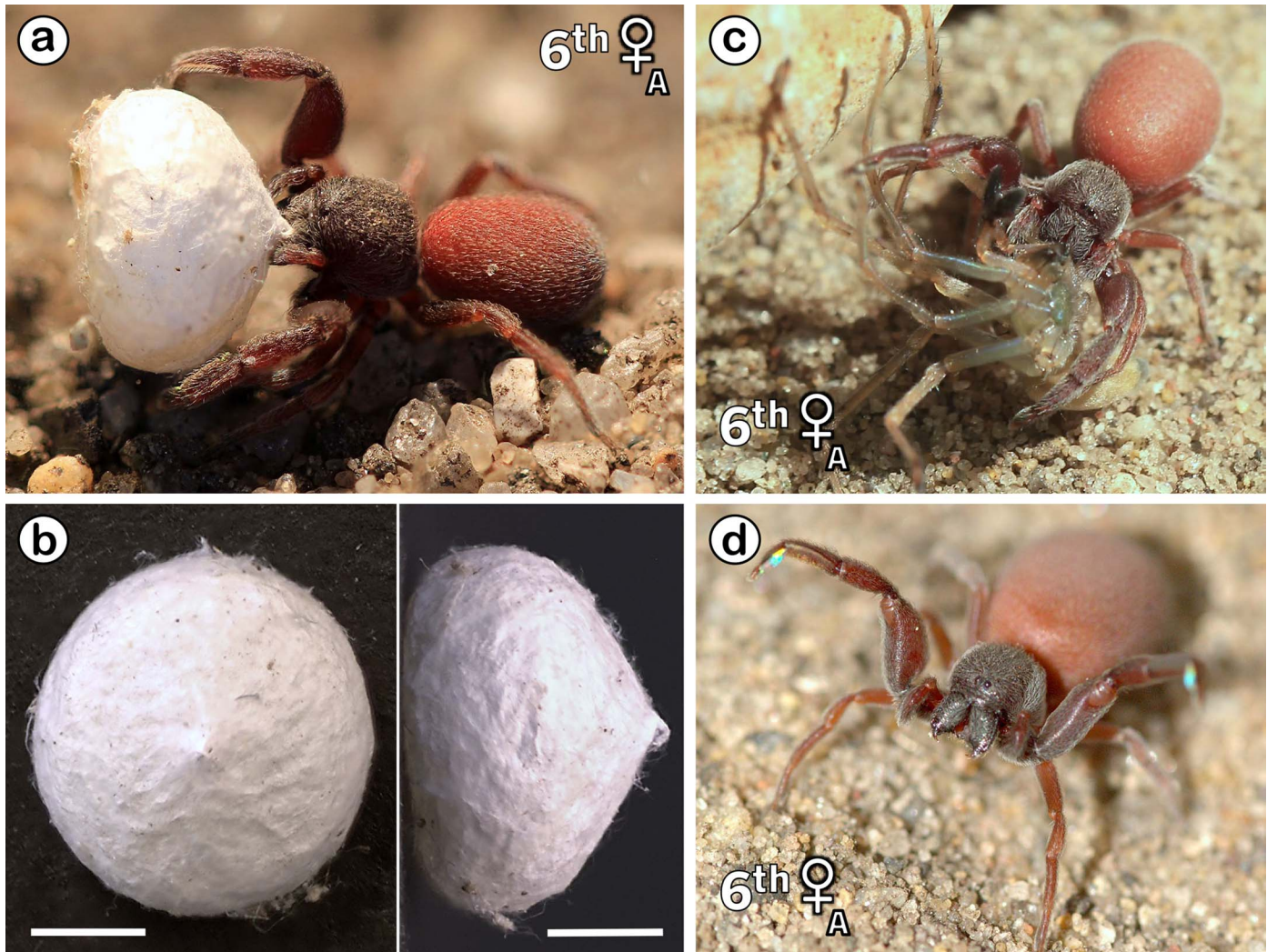


Figure 2.—Live adult female *Palpimanus uncatus*. (a) Specimen MCZ\_IZ\_163566 with field-built egg sac; both found on underside of rock by LM Newton. (b) Same egg sac in top (left) and side (right) views. What I call the bottom of the egg sac is on the left in the side view. Scale bars = 2 mm. (c, d) Specimen UNHC\_0049452 preying upon adult male *Cheiracanthium mildei* L. Koch, 1864 and in defensive posture (Uhl & Schmitt 1996; Penney 2009), respectively. A video of this female doing abdomen lifts after capturing this *C. mildei* is available (Watts & Townley 2022). Photo credits: (a, c) Pat Watts, (d) Scott Gasperin.

2 years seems likely: one male (MCZ\_IZ\_163565) collected as an adult on 15 May 2014 died just under 16 months later on 11 September 2015, and four males (MCZ\_IZ\_163560, UNHC\_0049453, UNHC\_0049458, one not deposited) collected as 4<sup>th</sup> instars in mid-May 2014, that became adults about 4 months later, were preserved in ethanol about 18 months after collection while still apparently healthy.

**Species identity.**—Ten of the captured specimens died before reaching maturity and thus their species identities are not certain. However, palps of all male adults and epigyna and internal genitalia of all female adults coincided with the images shown in Fig. 3 and Fig. 4, respectively, consistent with a *P. uncatus* identity. Moreover, *P. uncatus* is the only palpimanid species thus far known from Chios (Russell-Smith et al. 2011) and from nearby locations of Lesbos (Lesvos) (Bosmans et al. 2009) and İzmir Province in Türkiye (Lecigne 2011; Tutar & Yağmur 2023). Thus, while acknowledging uncertainty, I presume that most, if not all, of the immature field-collected specimens are also *P. uncatus* and their spinneret data are here combined with those of the better substantiated specimens.

Using autofluorescence emission from female genitalia preparations, sclerotized and unsclerotized structures could be distinguished based on their primary emissions, in the ranges 663–738 nm and 425–475 nm, respectively. In Fig. 4d,f,i, sclerotized (or sclerotin-like) and unsclerotized structures have been pseudocolored pink and green, respectively. The former included pore plates on spermathecae (Fig. 4h,i) and small distal patches on the grape-shaped glands (Fig. 4f,i) that at higher magnification were generally ring-shaped structures (not shown) reminiscent of ring structures visible on pore plates (Fig. 4i).

**Spinneret region overview.**—The tracheal spiracle opened a short distance (about 0.1–0.2 mm) anterior to the ALSs (Figs. 5a–c, 7b). No colulus or clear remnant of one was present (Figs. 5, 7d). By SEM, ALSs appeared two-segmented (but see Discussion), with the apical segment, bearing PI and MaA spigots and tartipores, much smaller than the basal segment (Figs. 5, 7e). Because the posterior spinneret region (PS) was typically compressed in spinneret preparations along the anterior-posterior axis, the well-developed



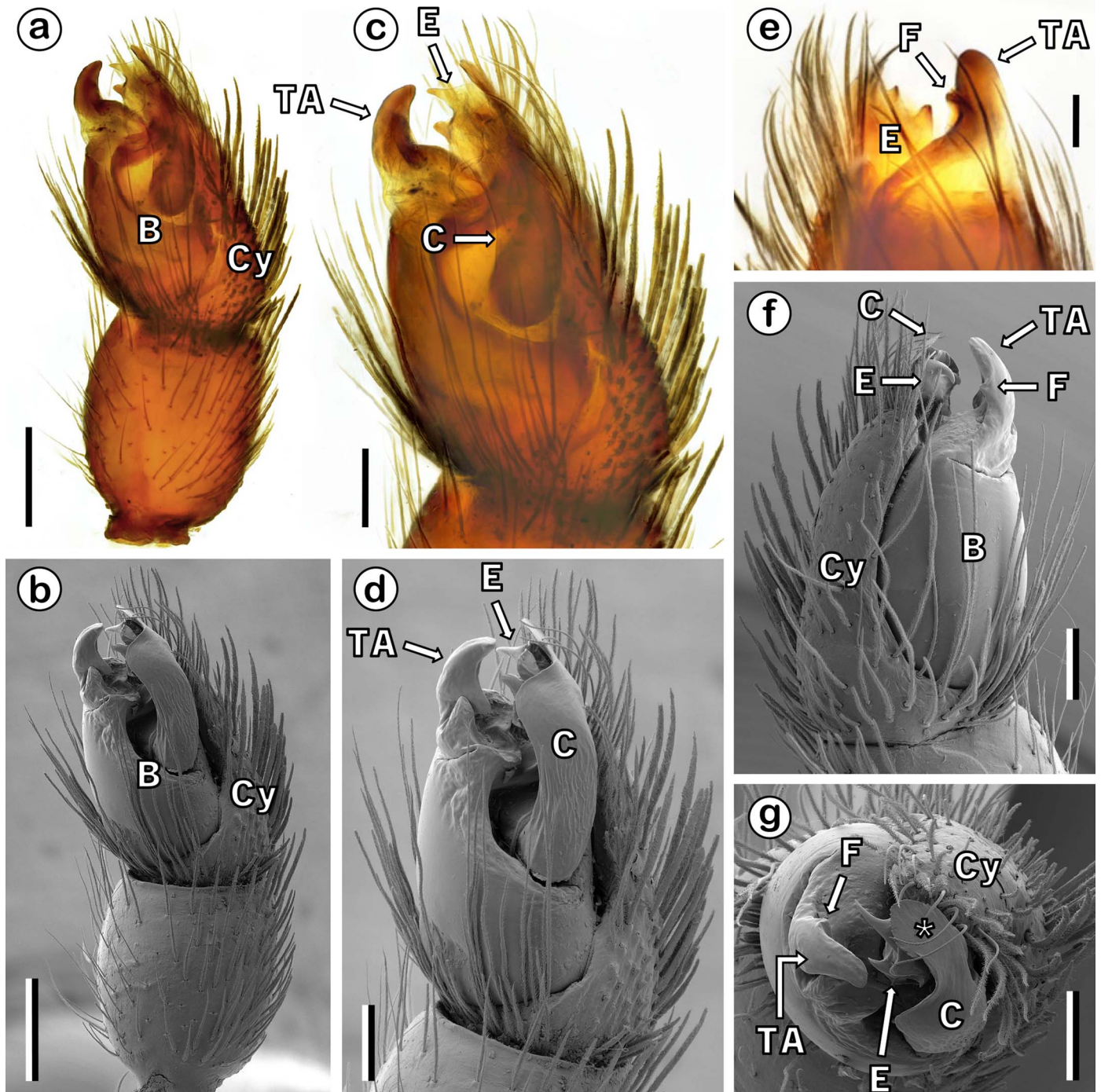


Figure 3.—Left male pedipalp of *Palpimanus uncatus*. (a, b) Tibia, cymbium (Cy), and bulb (B), ventral view. (c, d) Cymbium and bulb, ventral view. (e) Distal bulb, tilted dorsal view. Note retrolateral flange (F) (Platnick 1981) on tegular apophysis (TA). (f, g) Cymbium and bulb, dorsal and apical views, respectively. Note in (g) that conductor (C) has a dorsal lobe (\*), partly visible in (f). (a, c, e) TL; (b, d, f, g) SEM. (a–d, f, g) Specimen MCZ\_IJ\_163565; (e) Specimen UNHC\_0049453; both 6<sup>th</sup> instars. Identifications of sclerites follow Jocqué & Dippenaar-Schoeman (2006) and Hernández-Corral & Ferrández (2017). E, embolus. Scale bars: (a, b) 200  $\mu$ m; (c, d, f, g) 100  $\mu$ m; (e) 50  $\mu$ m.

ALSs were only slightly anterior to the anal tubercle (Figs. 5, 14b,e, f,h,i, 15a–c). In postembryos, however, the PS occupied an area of cuticle comparable to that of the ALSs (Fig. 7b), producing an arrangement of ALSs relative to the anal tubercle as in a typical araneomorph spider. The flat, hemi-elliptical PS of postembryos was in accord with an ancestry that included PLSs and PMSs, and the

separation it created between ALSs and anal tubercle resulted in pharate 1<sup>st</sup> instars with a less compressed PS than was observed subsequently (Figs. 7d, 14a).

A conspicuous feature of all instars was a single palisade-like row of long setose setae along the medial face of each ALS (Figs. 8a, b, 9a,d, 10a,d). Similar setae with numerous and relatively long



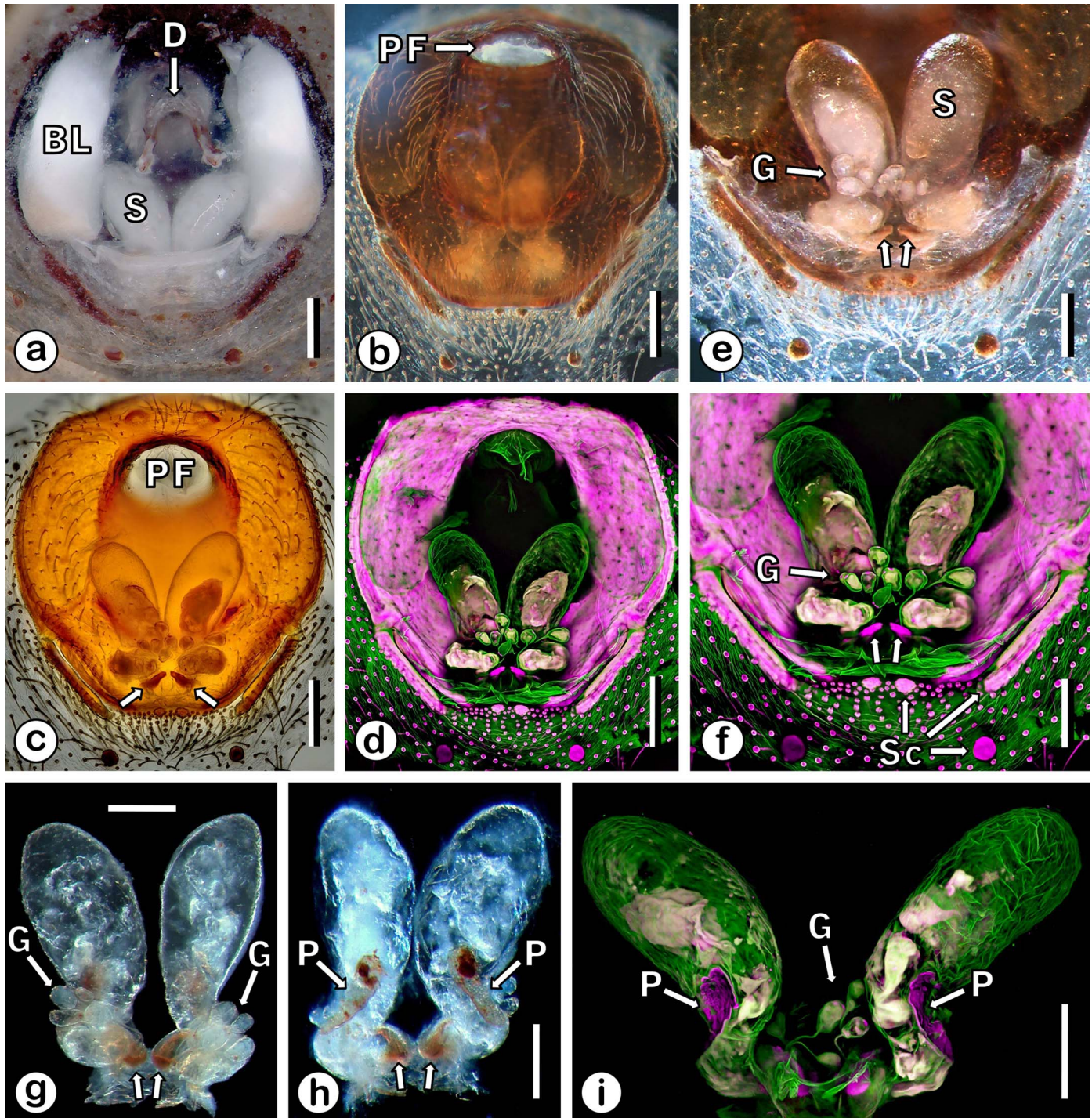


Figure 4.—Female genitalia of *Palpimanus uncatus*. (a–d) Abdominal scutum, small posterior sclerites, and genitalia. (a) Dorsal view of internal genitalia with book lungs (BL), dorsal posterior sclerite of pedicel (D) (with branched apodemes) (Ramírez 2014; Cala-Riquelme et al. 2018), and other tissues in situ. Ventral (b) and dorsal (c, d) views of the same region following removal of most non-genital components. (e, f) Internal genitalia and small post-scutal sclerites (Sc), dorsal view. Note cluster of grape-shaped glands/receptacula (G) on narrow stalks, presumably ducts (Platnick 1981; Forster & Platnick 1984; Marusik & Guseinov 2003; Zonstein & Marusik 2019; Prajapati et al. 2021; Zamani & Marusik 2021). (g–i) Isolated internal genitalia, dorsal (g) and ventral (h, i) views. Pore plates (P) visible in ventral view. Spermathecae in (i) artificially spread apart. Pair of unlabeled arrows in (c, e–h) point to diagnostically useful sclerotized structures (Platnick 1981). (a) RL, stereomicroscope; (b, g, h) TL, darkfield, stereomicroscope; (c) TL, brightfield, compound microscope; (d, f, i) 4-channel CLSM epi-autofluorescence; (e) RL + TL, darkfield, stereomicroscope. (a) Specimen MCZ\_IZ\_163566; (b–f, i) Specimen UNHC\_0049456; (g, h) Specimen UNHC\_0049452; all 6<sup>th</sup> instars. PF, pedicel foramen; S, spermatheca. Scale bars: (a–d) 300  $\mu$ m; (e–i) 200  $\mu$ m.



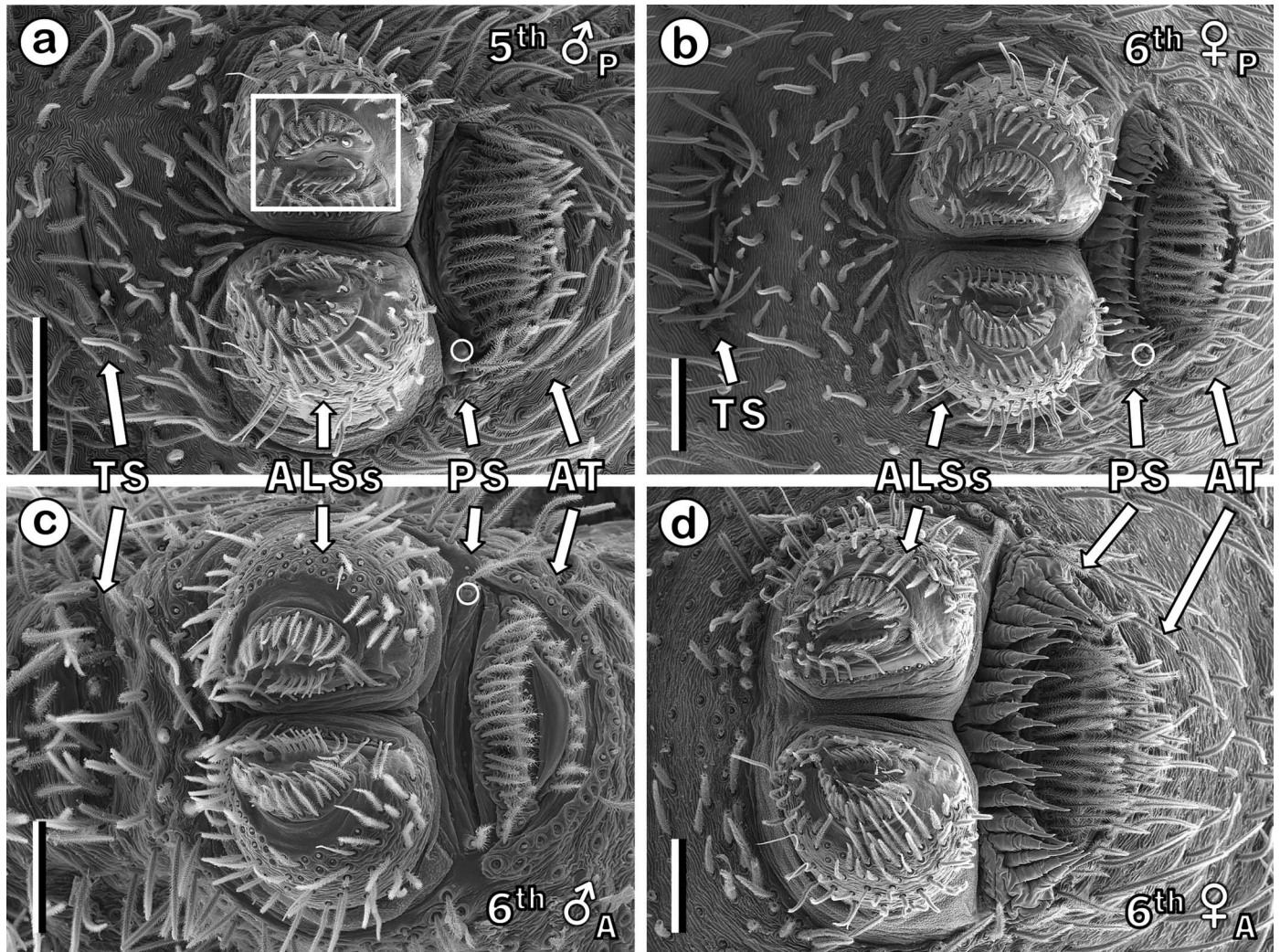


Figure 5.—Overview of spinnerets, tracheal spiracle (TS), and anal tubercle (AT) in male (a, c) and female (b, d) penultimate instars (subadults) (a, b) and adults (c, d) of *Palpimanus uncatius*. Boxed region in (a) indicates approximately the region presented in colorized Figs. 7f, 8a–d, 9a–c, 10a–d, and 11a,b; in fact, Fig. 11b is the same spinneret. Circles in (a–c) indicate locations of circular structures (disks) of unknown nature and function, shown in greater detail in Fig. 14. TS is just out of view in (d). PS bears CY spigots in females only, from 4<sup>th</sup> to adult (6<sup>th</sup> or 7<sup>th</sup>) stadia. (a) Specimen MCZ\_IZ\_163563; (b) Specimen MCZ\_IZ\_163557; (c) Specimen MCZ\_IZ\_163565; (d) Specimen MCZ\_IZ\_163556. Scale bars = 100  $\mu$ m.

bristles were abundantly distributed on and near the ALSs but those forming the medial row on ALSs were generally less densely covered with bristles and had longer bristle-free proximal portions.

**ALS spinning field description.**—No spigots occurred on the ALSs or PS of postembryos (Fig. 7b,c; Table 1). Unexpectedly, however, a single structure with tartipore-like morphology was present on each ALS of postembryos (Fig. 7c). A similarly positioned structure on each ALS of 1<sup>st</sup> instars was even more clearly of tartipore character (Figs. 7d–f, 8a, 12e). However, as neither structure was preceded by any spigots in earlier stages, it would seem neither had an opportunity to function as a tartipore. Thus, I identify both as tartipore primordia, as applied earlier (Townley & Tillinghast 2009; Townley & Harms 2017).

Beginning with 1<sup>st</sup> instars, a departure from the ALS spinning fields of most araneomorphs was apparent in the form of a spigot that consisted of multiple shafts on a common base (medial yellow in Figs. 7d–f, 8a; uncolored in Fig. 12e). From the 2<sup>nd</sup> stadium (Fig. 8b), the arrangement of this multi-shaft spigot with the other spigots and

tartipores on the ALS left little doubt that the multi-shaft spigot was, as Murphy & Roberts (2015) concluded, a modified MaA spigot. Specifically, it was apparently the 2<sup>o</sup> MaA spigot, making the relatively massive tartipore just lateral to it (large yellow in Fig. 8b) a 2<sup>o</sup> MaA tartipore, and the tartipore primordium present in postembryos and 1<sup>st</sup> instars a 2<sup>o</sup> MaA tartipore primordium (Figs. 7c–f, 8a, 12e). It may be that these primordia of postembryos and 1<sup>st</sup> instars are specifically associated with the developing odd-stadia and even-stadia sets of 2<sup>o</sup> MaAs, respectively, but this has not been established.

In addition to one multi-shaft 2<sup>o</sup> MaA spigot, 1<sup>st</sup> instars had one 1<sup>o</sup> MaA spigot per ALS (Figs. 7f, 8a, 12e) and this combination did not change during the spider's ontogeny, though the number of shafts on the 2<sup>o</sup> MaA spigot's common base gradually increased (Table 1). 1<sup>st</sup> instars also had two PI spigots per ALS, and the first PI tartipores, one per ALS, then appeared in 2<sup>nd</sup> instars (Fig. 8b). These PI structures also gradually increased during development with up to 7 and 12 PI spigots per ALS observed in male and female adults, respectively (Table 1). These modest numbers of PI spigots are consistent



with Wolff et al.'s (2021) observations that attachment discs in *P. gibbulus*, presumably used to secure MaA silk to substrates, are small, circular, and few. No attempts were made during this study to observe attachment discs but PI fibers were observed emerging from PI spigots on one exuvium (see below and Fig. 13a,b).

It was instructive to compare the ALS of *P. uncatius* with that of other, more typical CY Spigot clade taxa. I present one such comparison in Fig. 9e,f, showing the apical segment of an ALS from an exuvium shed by a male *A. aurantia*. It can be compared to any of the *P. uncatius* ALS apical segments shown in Figs. 7–11 but is most directly comparable to that shown in Fig. 9b, from an exuvium depicting the same stadium and sex as the *Argiope* Audouin, 1826 example. By the spigot and tartipore identities inferred in this report, similarities between the ALSs of *Argiope* and *Palpimanus* included (1) medially placed MaA spigots with the 1° MaA spigot anterior to the 2° MaA spigot and the 2° MaA tartipore lateral to the 2° MaA spigot, (2) laterally placed PI spigots interspersed with PI tartipores, and (3) a series of pores on the MaA spinning field that extended from lateral and anterior to the 1° MaA spigot to medial to the 2° MaA spigot. This last feature, shown in Fig. 9f (*Argiope*) and Fig. 12d–f (*Palpimanus*), indicated the presence of mechanoreceptors (Gorb & Barth 1996; Barth 2002). Consistent with this interpretation, at higher magnification, a putative dendrite attachment site could often, though not always, be seen within a pore (Fig. 12g–j). Differences between *Argiope* and *Palpimanus* included (1) a uni-shaft versus multi-shaft 2° MaA spigot, respectively, (2) PI spigots and tartipores tending to form a cluster rather than a slightly curved linear array, respectively, and (3) distinct setal morphologies.

This comparison using exuvia highlighted another similarity between the two genera. On exuvia from *Argiope* (Fig. 9f) and a few other examined entelegyne taxa (see Discussion), we have often observed a silk fiber emerging from each 2° MaA spigot. Likewise, I observed silk fibers emerging from the inferred 2° MaA spigots on exuvia from *P. uncatius*, except that there were, in many instances, multiple fibers issuing from an individual multi-shaft 2° MaA spigot (Figs. 8a, 9a,b,d, 10a, 11a, 12b,c; Table 1). Of 25 *P. uncatius* exuvia examined, 20 had silk fibers emerging from the 2° MaA spigots on both ALSs and another 4 had such fibers on one ALS. No exuvia had silk issuing from the inferred 1° MaA spigot, consistent with a non-T-A developmental mode. Of the 44 ALSs (from 24 exuvia) with silk, 38 had multiple silk fibers ( $\geq 2$ ) issuing from the 2° MaA spigot, with up to 14 silk fibers from a single 2° MaA spigot in later instars. Fig. 9d, which shows silk emerging from both 2° MaA spigots on one exuvium, demonstrates the substantial bundle of fibers that can be drawn by late instars.

Table 1 gives the proportion of 2° MaA shafts on exuvia that had emerging silk fibers, separated by stadium and, if known, sex. Overall, about half of these shafts on exuvia had silk fibers. Importantly, on five ALSs involving four exuvia ( $\text{♀} + \text{♂}$ ) I found that *P. uncatius* were capable of drawing silk from all shafts on a 2° MaA spigot during proecdysis and ecdysis. These exuvia represented 4<sup>th</sup> and 5<sup>th</sup> instars and had 9–14 shafts per 2° MaA spigot, all with emerging silk fibers (Table 1). Thus, all ducts that connect to shafts on 2° MaA spigots must be T-A. That this accommodation is accomplished by the single large 2° MaA tartipore was documented to some extent in three *P. uncatius* that were close to ecdysing at the time of death. In these individuals, I examined old and new (pharate) exoskeletons separately and the latter exhibited multiple 2° MaA ducts encircled by the single 2° MaA tartipore. The two best examples are shown in Fig. 10e,f (the ALS in Fig. 10e

is also shown at lower magnification in Fig. 10d). Interestingly, within each 2° MaA tartipore, the enzymatic cleaning employed during spinneret preparation (see Methods) appeared to unravel cuticular linings of different 2° MaA ducts to different degrees, with some duct linings essentially intact and others so distorted as to be almost unrecognizable (Fig. 10e,f).

Shaft morphology differed between 1° and 2° MaA spigots in both sexes. The former tended to taper distally more than the latter, allowing for endpieces on 2° MaA shafts that were usually larger and more elongated than those of 1° MaA shafts (Fig. 12d,e). The cross-sectional shape of silk fibers emerging from 2° MaA shafts on exuvia varied from nearly circular to ribbon-like but was typically somewhat flattened (Fig. 12b,c), apparently reflecting the elongated, slit-like endpieces on these shafts (Fig. 12a). An analogous disparity to that seen between 1° (non-T-A) and 2° (T-A) MaA spigot shafts was noted between non-T-A and T-A PI spigots in both sexes: T-A PI spigots tended to have larger and more elongated endpieces and openings than non-T-A PI spigots (Fig. 13d).

Apart from the 2° MaA silk fibers that were emerging on many exuvia, the only other silk fibers observed issuing from any spigots were PI fibers on both ALSs on a single exuvium, again indicating use during ecdysis. These were emerging from two of four T-A PI spigots on each ALS (Fig. 13a,b). Confirmation that some PI ducts were indeed T-A was most clearly illustrated in pharate exoskeletons of proecdysial spiders where, just as with 2° MaA ducts (Fig. 10e,f), cuticular linings of PI ducts sometimes remained in situ throughout the spinneret preparation protocol (with some unraveling due to enzymatic cleaning). These cuticular linings were encircled by PI tartipores, one duct per tartipore (Fig. 13c).

**PS description.**—I could not discern ancestral borders of PLSs and PMSs within the PS by SEM. From the 1<sup>st</sup> stadium, the PS was laterally bookended by small elevations surmounted by 1–2 setose setae (Figs. 7d, 14, 15a–c). These setae, like those associated with the anal tubercle, had longer, more extended bristles than the setose setae that form the main ALS setal type.

Just medial to these PS setae, a round to elliptical structure ('disk') was observed on 31 of 66 specimens (exuvia or spiders) of 1<sup>st</sup> to adult instars, male and female (though none seen on adult females). On some specimens, this disk was apparent on both sides of the PS (Fig. 14a–d;  $n = 15$ ); on others, it was evident on only one side, left or right (Figs. 5a–c, 14e–i;  $n = 16$ ). Note in Fig. 14h,i that this disk was apparent on the right side only on two consecutive exoskeletons of the same individual: one of three such occurrences of consecutive 'right-side-only' disks. No examples were seen of consecutive 'left-side-only' disks but there were four occurrences of consecutive 'both-sides' disks involving three spiders. Views were obstructed in five of 35 specimens on which no disks were seen, and in four of 16 specimens on which one disk was seen, and were thus likely responsible for some missed disks. Incidence of disks was strongly skewed toward earlier instars: at least one disk was observed on 22 of 24 specimens (92%) representing 1<sup>st</sup> to 3<sup>rd</sup> instars, but on only 9 of 42 specimens (21%) representing 4<sup>th</sup> to 7<sup>th</sup> instars. What the disks represent is currently unknown.

Among adults, spigots on the PS appeared to be of a single type and occurred only in females (Figs. 5c,d, 15c,e,f). Thus, a CY spigot identity appears most likely and I designate them as such here. CY spigots in 4<sup>th</sup> instars emerged directly from the surrounding cuticle (Fig. 15d). In penultimate instars, CY spigots tended to sit atop a short, flexible cuticular cone or cylinder (Figs. 5b, 15b). This flexible and probably hydrostatically inflatable pedestal

(indicated by differing degrees of inflation noted among CY spigots in one female) seemed further lengthened in adults: inflated, it was comparable in height to the spigot, if not longer (Figs. 5d, 15c,e).

**Ontogenetic changes in spigot (or spigot shaft) and tartipore numbers.**— $2^\circ$  *MaA* spigot shafts The number of shafts on each  $2^\circ$  *MaA* spigot tended to increase during development from a low in  $1^{\text{st}}$  instars of 3 (Fig. 12e) to a high in female adults of 23 (not shown, though a specimen with 22 is shown in Fig. 10d). Sexual dimorphism was apparent, with the mean number of shafts rising in each successive stadium in females, but in males rising through the  $5^{\text{th}}$  (penultimate) stadium only and then showing a 14% mean decline after the final molt (Table 1). Thus, the largest number of  $2^\circ$  *MaA* spigot shafts in males, 14, occurred in a penultimate ( $5^{\text{th}}$ ) instar (Fig. 9d, R ALS).

Data from consecutive exoskeletons in four males made it possible to consider this decrease in number of  $2^\circ$  *MaA* spigot shafts in late males at the individual level. One comparison of interest was between consecutive penultimate ( $5^{\text{th}}$ ) and adult ( $6^{\text{th}}$ ) stadium exoskeletons from these four males (2 ALSs/male, 8 ALSs total). This showed that on two ALSs (from different individuals) there was no change in shaft number following the last molt, while on the other six ALSs there were declines of 1–5 shafts per  $2^\circ$  *MaA* spigot. However, because  $2^\circ$  *MaAs* are T-A, this was a comparison between two entirely different groups or sets of  $2^\circ$  *MaAs* that functioned in alternate stadia (an odd-stadia set and an even-stadia set, see Terminology). More meaningful to an appreciation of silk gland dynamics was a comparison between antepenultimate ( $4^{\text{th}}$ ) and adult ( $6^{\text{th}}$ ) stadium exoskeletons from these four males; i.e., a comparison *within* the even-stadia set of  $2^\circ$  *MaAs*. By this comparison, on five ALSs shaft numbers increased by 1–2 shafts per  $2^\circ$  *MaA* spigot from the antepenultimate to the adult stadium, two did not change, and only one actually decreased (by 1 shaft). The left ALS spinning field on antepenultimate, penultimate, and adult stadium exoskeletons from one of these four males is shown in Fig. 9a–c where color coding helps emphasize that the  $2^\circ$  *MaAs* in use during the penultimate stadium (Fig. 9b) were different from the  $2^\circ$  *MaAs* in use during the antepenultimate and adult stadia (Fig. 9a,c).

*PI spigots and tartipores* Ontogenetic increases in PI spigots and tartipores followed a pattern (henceforth ‘standard pattern’) that was invariably observed from the  $1^{\text{st}}$  through  $3^{\text{rd}}$  stadia and was still evident overall during later stadia, though deviations from the standard pattern, especially in females, increased on average over successive stadia. Beginning with two PI spigots and no PI tartipores per ALS in  $1^{\text{st}}$  instars (Figs. 7f, 8a), the standard pattern was for the number of both structures to increase by one per ALS with each molt (Table 1). As detailed below, this increase of one PI spigot and one PI tartipore per ALS per molt is actually attained by the addition of two PIs per ALS to either the odd-stadia set or even-stadia set of PIs, in alternating stadia, and these two new PIs associated with each ALS are of the T-A subtype.

$4^{\text{th}}$  instars that exhibited the standard pattern had five PI spigots per ALS. This was observed on 16 of 18 male ALSs (89%) and on 9 of 12 female ALSs (75%). The expected three PI tartipores were present on all 18 male ALSs and on 10 of 12 female ALSs (83%). Though the number of PI spigots was invariably four in seven  $3^{\text{rd}}$  instars (Table 1), occasional  $4^{\text{th}}$  instars with two PI tartipores (the 2 non-standard female ALSs) rather than three indicated that occasional  $3^{\text{rd}}$  instars with three PI spigots can be expected in the population.

$5^{\text{th}}$  instars that presented the standard pattern had six PI spigots per ALS and this was seen on 9 of 12 male ALSs (75%) and on 5

of 12 female ALSs (42%). Notably, five deviations from the standard pattern were larger numbers of PI spigots (7 or 8) present only in (3) females. The expected four PI tartipores per ALS were present on 10 of 12 ALSs (83%) in both males and females.

$6^{\text{th}}$  instars that showed the standard pattern had seven PI spigots per ALS, as seen on 6 of 10 adult male ALSs (60%), but on only 4 of 17 female ALSs (24%), all but two adult. Again, 12 deviations from the standard pattern were larger numbers of PI spigots (8 to 11) present only in females. The expected five PI tartipores per ALS were present on 9 of 10 male ALSs (90%) and on 10 of 16 female ALSs (63%), with five deviations being a larger number of PI tartipores (6 to 8) restricted to (3) females.

If *P. uncatus* invariably adhered to the standard pattern throughout ontogeny, the number of non-T-A PI spigots per ALS at all stadia would be guaranteed to be one. But as just detailed, deviations from the standard pattern were observed from the  $4^{\text{th}}$  stadium and tended to increase subsequently. Nevertheless, in all instances evaluating  $1^{\text{st}}$  to  $6^{\text{th}}$  instars, when two consecutive exoskeletons from the same individual were examined ( $n = 28$  pairs of consecutive exoskeletons) and the number of PI spigots in the earlier exoskeleton was compared with the number of PI tartipores in the later exoskeleton, spigot number per ALS invariably exceeded tartipore number by one. Thus, the inferred number of non-T-A PI spigots was also invariably one per ALS at all stadia (Table 2).

I identified each PI spigot as serving either the non-T-A PI or a T-A PI by comparing arrangements of PI spigots and tartipores from stadium to stadium and identifying the scenario that seemed to best account for the observed arrangements. In the same way, for each T-A PI and its spigot, I determined the stadium in which that PI was first used. The color-coded results of this approach are presented in Figs. 7–11 with a key in Fig. 6. Among the results, the inferred location of the single non-T-A PI spigot on each ALS, colored red, was consistent throughout all stadia: anterior to all other PI spigots.

For spiders displaying the standard pattern (T-A PI spigots and PI tartipores each increase by one per ALS following each molt) (Figs. 8, 9a–c, 11a), developmental changes in PI spigot and tartipore arrangements followed a stereotypic sequence that was apparent from the  $2^{\text{nd}}$  stadium forward. In the  $1^{\text{st}}$  stadium one T-A PI per ALS constituted the entire odd-stadia set of T-A PIs and the spigot serving this PI on each ALS is colored yellow in Figs. 7f and 8a. Thereafter, a new pair of T-A PIs per ALS was added, in alternating stadia, to either the even-stadia set or odd-stadia set of T-A PIs. The spigots serving the new pair were located at either end, anterior and posterior, of a line of PI tartipores/spigots representing earlier-formed T-A PIs. In  $2^{\text{nd}}$  instars, that ‘line’ actually consisted of only a single PI tartipore (small yellow tartipore, Fig. 8b), representing the T-A PI used during the  $1^{\text{st}}$  stadium, and the new pair of T-A PIs per ALS, served by the blue PI spigots in Fig. 8b, constituted the entire even-stadia set of T-A PIs up to that point. In  $3^{\text{rd}}$  instars, the line on an ALS representing earlier-formed T-A PIs consisted of one PI spigot (yellow, Fig. 8c), marking a return to service for the T-A PI used during the  $1^{\text{st}}$  stadium, flanked by a pair of PI tartipores (small blue tartipores, Fig. 8c) representing the T-A PIs used during the  $2^{\text{nd}}$  stadium. The PI spigots at either end of this line (dark green, Fig. 8c) thus served the newly formed pair of T-A PIs within the odd-stadia set of T-A PIs. By the  $6^{\text{th}}$  stadium, the line consisted of four T-A PI spigots (blue & purplish-pink, Fig. 9c) and five PI tartipores (yellow, dark green & brownish orange, Fig. 9c), and the new members of the even-stadia set of T-A PIs were served by spigots at

	Silk gland molt condition <sup>a</sup>	Stadium when silk gland first used	Subsequent stadia when silk gland used (potentially) <sup>b</sup>
<b>R</b>	non-T-A	1 <sup>st</sup>	2 <sup>nd</sup> , 3 <sup>rd</sup> , 4 <sup>th</sup> , 5 <sup>th</sup> , 6 <sup>th</sup> , 7 <sup>th</sup>
<b>Y</b>	T-A	1 <sup>st</sup>	3 <sup>rd</sup> , 5 <sup>th</sup> , 7 <sup>th</sup>
<b>B</b>	T-A	2 <sup>nd</sup>	4 <sup>th</sup> , 6 <sup>th</sup>
<b>DG</b>	T-A	3 <sup>rd</sup>	5 <sup>th</sup> , 7 <sup>th</sup>
<b>PP</b>	T-A	4 <sup>th</sup>	6 <sup>th</sup>
<b>BO</b>	T-A	5 <sup>th</sup>	7 <sup>th</sup>
<b>LG</b>	T-A	6 <sup>th</sup>	none
<b>T</b>	T-A	7 <sup>th</sup>	none

<sup>a</sup>T-A = tarti pore-accommodated

<sup>b</sup>Assuming *Palpimanus uncutus* become adult no later than 7<sup>th</sup> stadium. R, red; Y, yellow; B, blue; DG, dark green; PP, purplish pink; BO, brownish orange; LG, light green; T, turquoise

Other figure conventions:

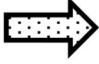
- 1)  A dotted arrow connects scans of the same spinneret or region in two consecutive exoskeletons from the same individual.
- 2) The instar depicted in an image is indicated by labels 1<sup>st</sup> through 7<sup>th</sup>, followed by ((Ex)) if spinnerets on an **exuvium** are shown and ((Ph)) if spinnerets on the **pharate** (new) cuticle of an individual close to ecdysing are shown. PE = **postembryo**.
- 3) The sex of the individual depicted in an image, if known, is given (♀, ♂) followed by a subscript: J (**juvenile**), P (**penultimate instar** = subadult), or A (**adult**).
- 4) To facilitate comparisons, scans that present a single ALS depict a **left ALS**. Anterior is at left, medial is at bottom. Scans of single right ALSs used in figures have been flipped horizontally in Microsoft® PowerPoint®, version 2105, to yield pseudo-left images. Figure legends state the true handedness.
- 5) Scans that contain both ALSs have the left ALS at top and anterior is at left.

Figure 6.—Key to color coding of silk gland spigots and tartipores in Figs. 7–11, using the procedure of Dolejš et al. (2014), and other conventions used in scans of spinnerets.

either end of this line (light green, Fig. 9c). Throughout these additions of new T-A PIs and their spigots, the single non-T-A PI spigot on each ALS (red, Figs. 7d–f, 8, 9a–c, 10a–d, 11a,b) appeared to retain its position anterior to all T-A PI spigots and tartipores, lateral to the 1° MaA spigot.

Deviations from the standard pattern, higher or lower, with respect to number of PI spigots were observed on 34 of 83 ALSs from 23 individuals as they existed during 4<sup>th</sup> to 7<sup>th</sup> stadia (PI tarti pore deviations also occurred, but these simply reflected PI spigot deviations from the preceding stadium). Nineteen of these ALSs had more PI spigots than the standard pattern predicted, resulting from additions of 3–6 T-A PIs per ALS, rather than two, to either the odd-stadia set or even-stadia set of T-A PIs. This occurred exclusively in females, with larger-than-standard PI spigot numbers appearing in some 5<sup>th</sup> and all 6<sup>th</sup> and (pharate) 7<sup>th</sup> instars, at least on one ALS (Fig. 10a–d; Table 1). Thus, these deviations were normal parts of female ontogeny. In these females, two of the new PI spigots occupied the same locations as in standard-pattern individuals, at anterior and posterior ends of the line of T-A PI spigots/tartipores, while the other new PI spigots appeared to form, primarily, medial to PI spigots serving earlier-formed T-A PIs. This resulted in the single-file line of PI spigots present in standard-pattern spiders, as in Figs. 8, 9a–c, being doubled in part, as in Fig. 10a–d.

The other 15 ALSs (18% of examined 4<sup>th</sup>–7<sup>th</sup> stadium ALSs) that showed deviations had fewer PI spigots than the standard pattern predicted, nine involving four males, six involving four females, and seemed to represent minor developmental abnormalities. Two causes appeared responsible for 11 of the 15 downward deviations. In four instances (involving 3 ♂), only one of the usual two new T-A PIs per ALS was added to the odd- or even-stadia sets of T-A PIs. In seven instances (involving 2 ♂, 2 ♀), it appeared that 1–2 T-A PIs that functioned in an earlier stadium did not return to service at their next opportunity to do so. An example of this is shown in Fig. 11, which begins with a standard pattern arrangement of PI spigots/tartipores on the 4<sup>th</sup> stadium ALS (Fig. 11a). The three PI tartipores in that scan, one yellow, two dark green, indicate that as a 3<sup>rd</sup> instar, this individual had four PI spigots, one non-T-A, three T-A, and would have looked like Fig. 8c. Normally, the three T-A PIs served by those three T-A PI spigots would return to service during the 5<sup>th</sup> stadium, with their spigots located between the two PI tartipores colored purplish pink in Fig. 11b, as seen in Fig. 9b. Instead, only one of the expected three spigots was present (colored dark green as a best guess in Fig. 11b but yellow was about equally likely given available information). However, two T-A PIs, new members of the odd-stadia set of T-A PIs and functioning for the first time in the 5<sup>th</sup> stadium, apparently formed normally as indicated by the brownish orange PI spigots in Fig. 11b at either end of the line of T-A PI spigots and tartipores. The mechanism by which the remaining four downward deviations (involving 1 ALS on each of 2 ♀ over two stadia) were produced was not clear but it appeared that the PI field on one ALS was developmentally one stadium behind the other. Unfortunately, the relevant spinnerets from earlier stadia for these individuals were not available.

CY spigots CY spigots first appeared in small numbers (≤ 6) and in single file in female 4<sup>th</sup> instars (Table 1; Figs. 14f, 15a,d), though in one female 4<sup>th</sup> instar (UNHC\_0049451) of six, such spigots were not present. It was only when she entered proecdysis and the exoskeleton of the pharate 5<sup>th</sup> instar formed that 14 CY spigots developed, the smallest number seen on a (pharate) 5<sup>th</sup> instar. Given this, there is the possibility that up to three of the nine 4<sup>th</sup> instars identified as males in Table 1 (because of an absence of CY spigots) were actually females since they did not live long enough to verify the absence of CY spigots during the 5<sup>th</sup> stadium: two died as 4<sup>th</sup> instars, one died as a 3<sup>rd</sup> instar containing the pharate 4<sup>th</sup> instar. A larger number of CY spigots in 5<sup>th</sup> instars gave the impression that the spigots could no longer fit from one lateral edge of the array to



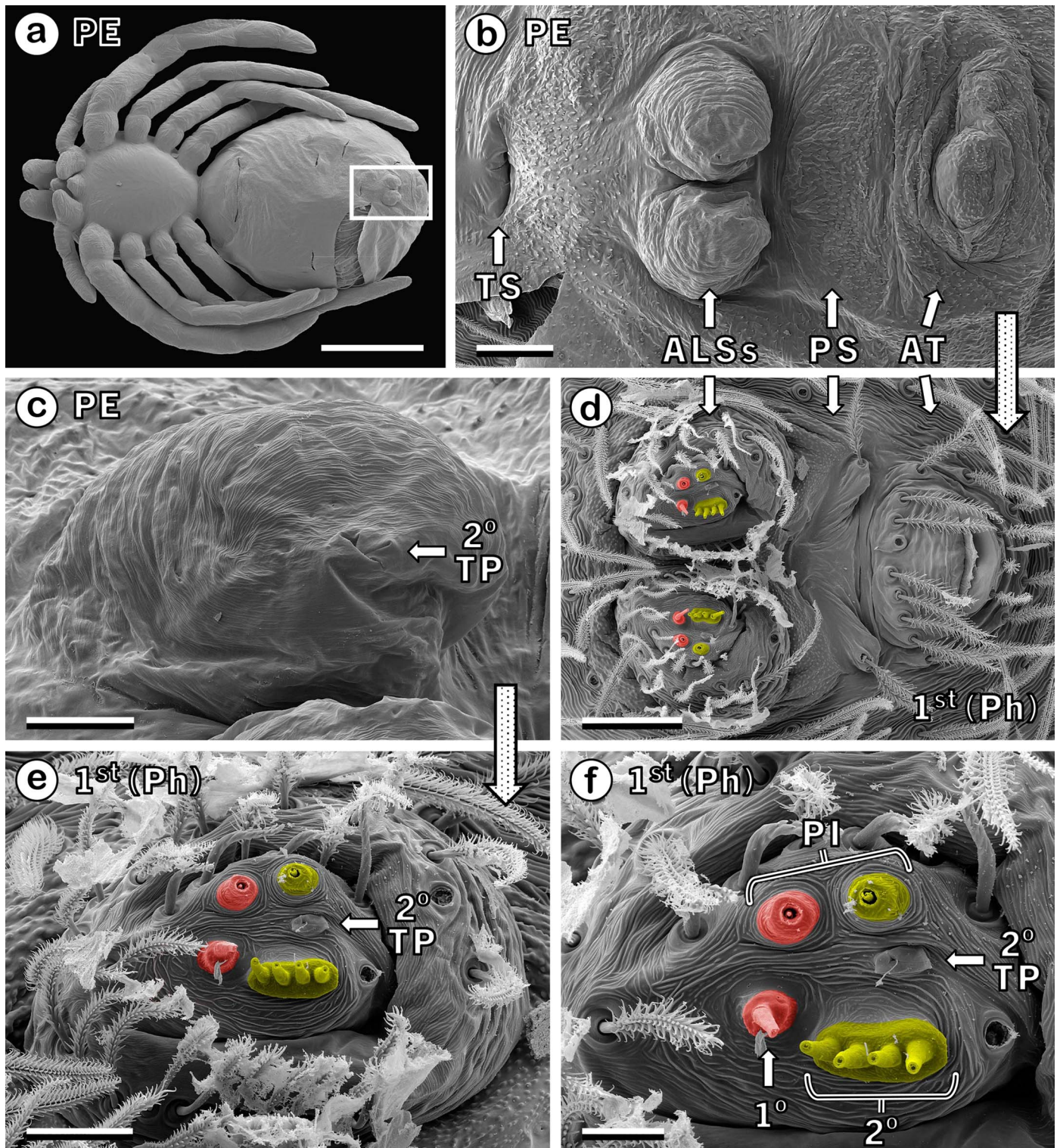


Figure 7.—Spinnerets on a postembryo (PE) of *Palpimanus uncutus* close to ecdysis and on underlying, new exoskeleton of pharate 1<sup>st</sup> instar. Progeny of Specimen MCZ\_IZ\_163558. (a) Overview of PE, ventral view. Tear in exoskeleton on opisthosoma, revealing new exoskeleton with setae beneath. Boxed region in (a) containing spinnerets, tracheal spiracle (TS), and anal tubercle (AT) shown at higher magnification in (b). (c) Same, higher magnification of left ALS. (d) Overview of spinnerets on pharate 1<sup>st</sup> instar after removing PE exoskeleton (an operation that resulted in all spigot shafts being partially or entirely broken off). (e) Same, left ALS. (f) Spinning field of left ALS. Color assignments (key in Fig. 6) based on observations of ALSs of 2<sup>nd</sup> instars (e.g., Fig. 8b). 1<sup>o</sup>, 1<sup>o</sup> MaA spigot; 2<sup>o</sup>, 2<sup>o</sup> MaA spigot; PI, PI spigots; 2<sup>o</sup> TP, 2<sup>o</sup> MaA tartipore primordium. Scale bars: (a) 500  $\mu$ m; (b, d) 50  $\mu$ m; (c, e) 20  $\mu$ m; (f) 10  $\mu$ m.



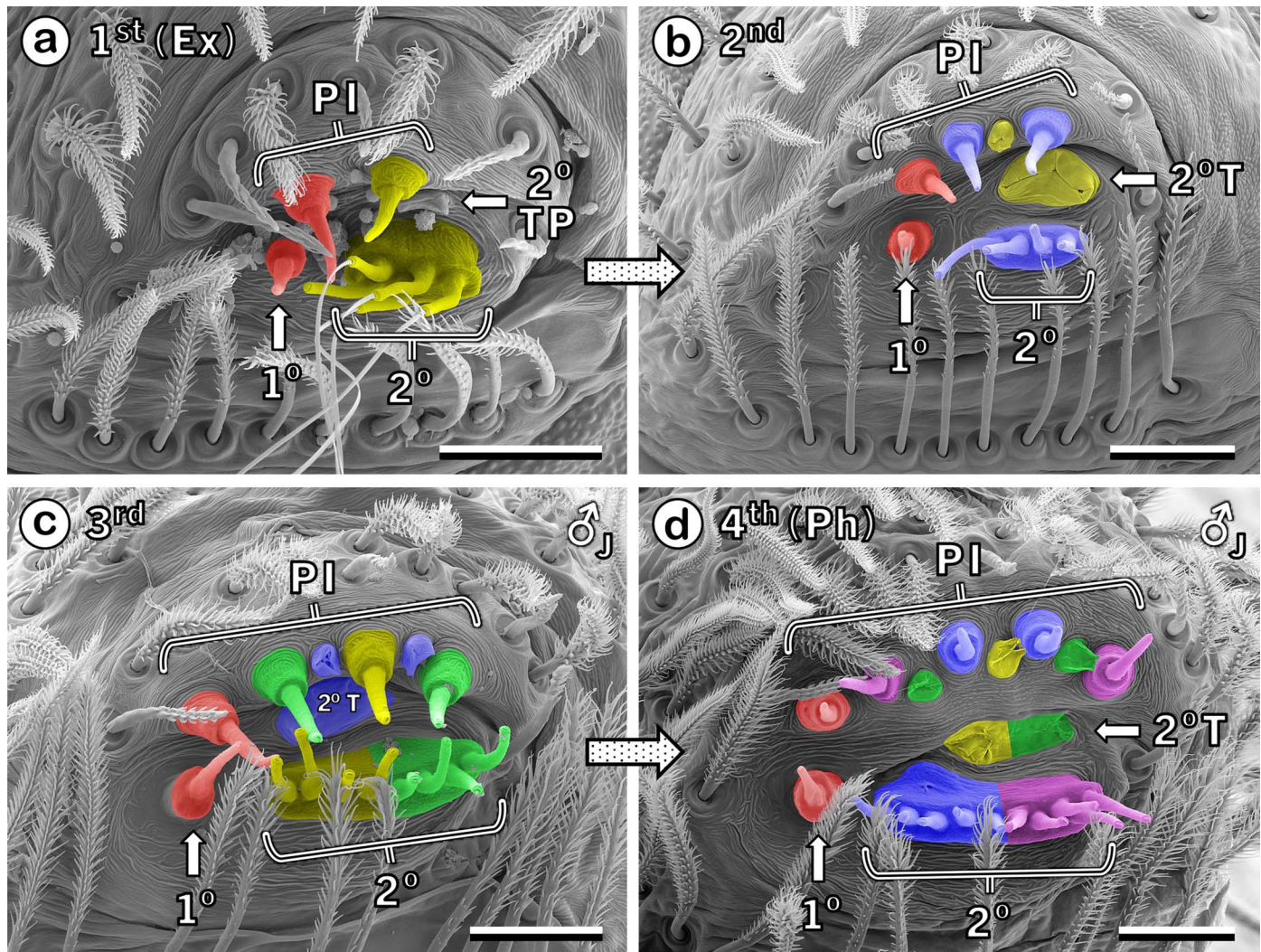


Figure 8.—Spinning fields on right ALSs (images flipped horizontally) of *Palpimanus uncatus*. (a) Most recent exuvium shed by the 2<sup>nd</sup> instar shown in (b). Note silk fibers emerging from shafts of 2° MaA spigot on exuvium, demonstrating use of 2° MaAs at ecdysis. (c, d) Male juvenile 3<sup>rd</sup> instar well into proecdysis, showing the same spinning field on old (c) and new (d) exoskeletons. (a, b) Specimen UNHC\_0049455; (c, d) Specimen MCZ\_IJ\_163559. 1°, 1° MaA spigot; 2°, 2° MaA spigot; PI, PI spigots and tartipores; 2° T, 2° MaA tartipore; 2° TP, 2° MaA tartipore primordium. Scale bars = 20 μm.

the other in single file and a partial to entire second row formed. Depending on the number of CY spigots in different 5<sup>th</sup> instars, there was a tendency, not strictly observed, for the second row to fill starting at the lateral ends of the array, progressing medially (Fig. 15b). In adults, a further increase in number of CY spigots (Table 1) resulted in the entire array being two to four spigots deep, anterior to posterior (Figs. 5d, 15c,e).

## DISCUSSION

**T-A and non-T-A PIs.**—This study began with an interest in exploring the phylogenetic distribution of a PI character state in which the number of non-T-A PIs associated with each ALS is fixed at two throughout ontogeny from the 1<sup>st</sup> stadium (Townley & Tillinghast 2009; Townley & Harms 2017). This state, revealed by PI spigot and tartipore data, has so far been observed only in representatives of three araneoid families (see introductory comments). As Araneoidea is nested within the CY Spigot clade (Wheeler et al.

2017), evaluating this character in more basal members of this clade is especially desirable and led to this examination of the spinnerets of *P. uncatus*, a member of Palpimanoidea. The result was unambiguous: as in the araneoids examined to date, *P. uncatus* have both T-A and non-T-A PIs and the number of non-T-A PIs per ALS is constant from the 1<sup>st</sup> stadium to the adult stadium. That number, however, is one per ALS in *P. uncatus* rather than two (Table 2). This difference may reflect smaller numbers of PIs overall in *P. uncatus* compared to the examined araneoids and/or reflect the atypical linear arrangement of PI spigots in *P. uncatus* compared to more clustered PI spinning fields (some with handle-like extensions) typical within the CY Spigot clade, including among araneoids (e.g., cf. Fig. 9b,e) (Coddington 1989; Platnick et al. 1991; Scharff & Coddington 1997; Griswold et al. 1998, 2005; Ramirez 2014). It will be of interest therefore to also evaluate this character in palpimanooids that exhibit a more clustered arrangement and/or a larger number of PI spigots, as in some Archaeidae, Huttoniidae (Platnick et al. 1991; Griswold et al. 2005; Murphy & Roberts 2015), Mecysmauchenidae (Platnick et al. 1991;



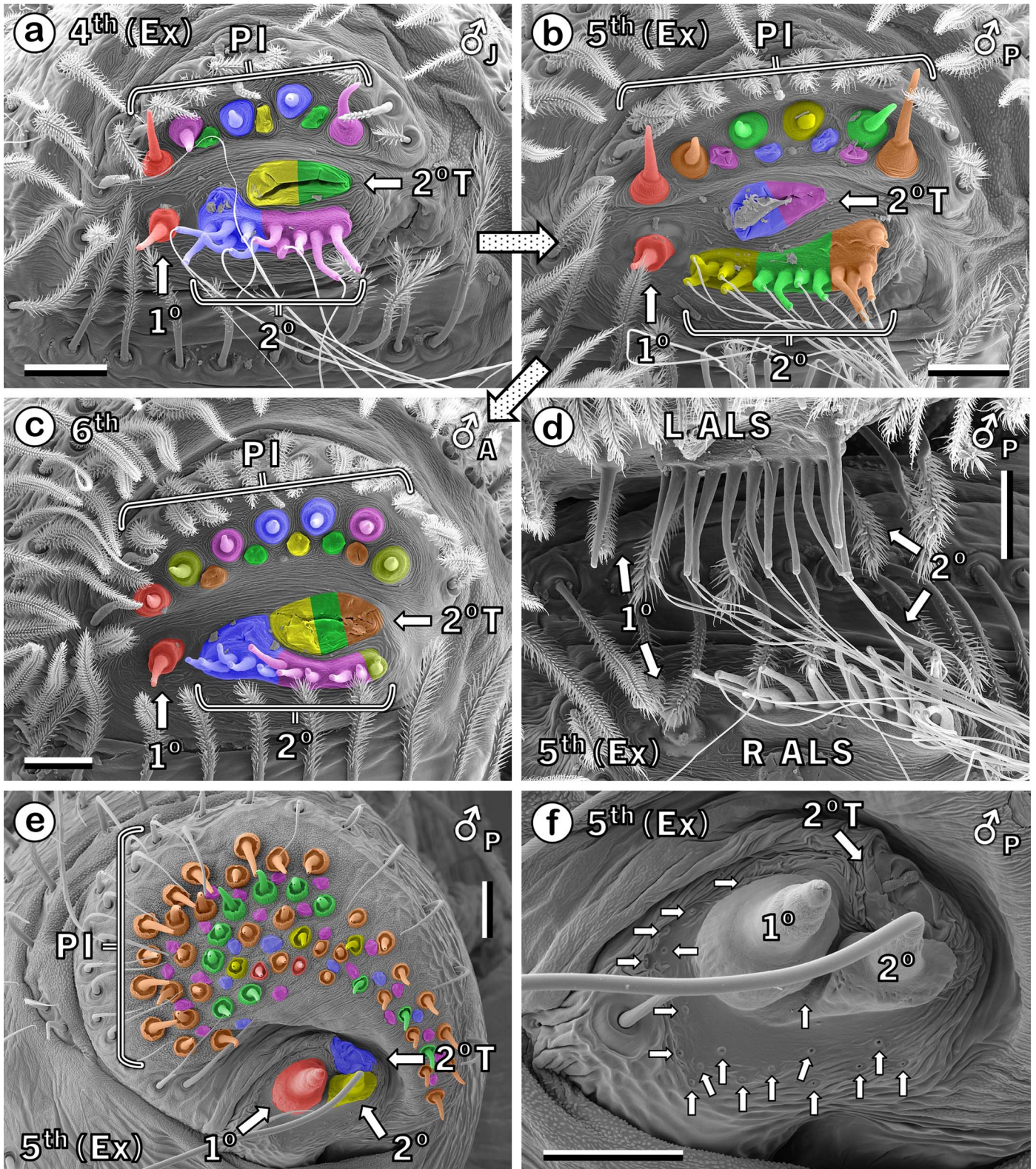


Figure 9.—Spinning fields on ALSs of *Palpimanus uncatus* (a–d) and *Argiope aurantia* (e, f). (a–b) Two most recent exuvia shed by the adult male 6<sup>th</sup> instar shown in (c). (a–c) Left ALS. (d) MaA spigots on right and left ALSs on the exuvium shown in (b). Note silk fibers emerging from shafts of 2° MaA spigots on exuvia (a, b, d). (e) ALS spinning field on final exuvium shed by male *A. aurantia*. (f) Same, higher magnification of MaA spinning field. Note silk fiber emerging from shaft of 2° MaA spigot and multiple pores in the field (unlabeled arrows) marking putative dendrite insertion sites of mechanoreceptors (Gorb & Barth 1996). Color coding in (e) was made possible by examining the preceding four exuvia shed by the same individual. (e, f) Right ALS (images flipped horizontally). (a–d) Specimen UNHC\_0049458. 1°, 1° MaA spigot; 2°, 2° MaA spigot; PI, PI spigots and tartipores; 2° T, 2° MaA tartipore. Scale bars = 20  $\mu$ m.



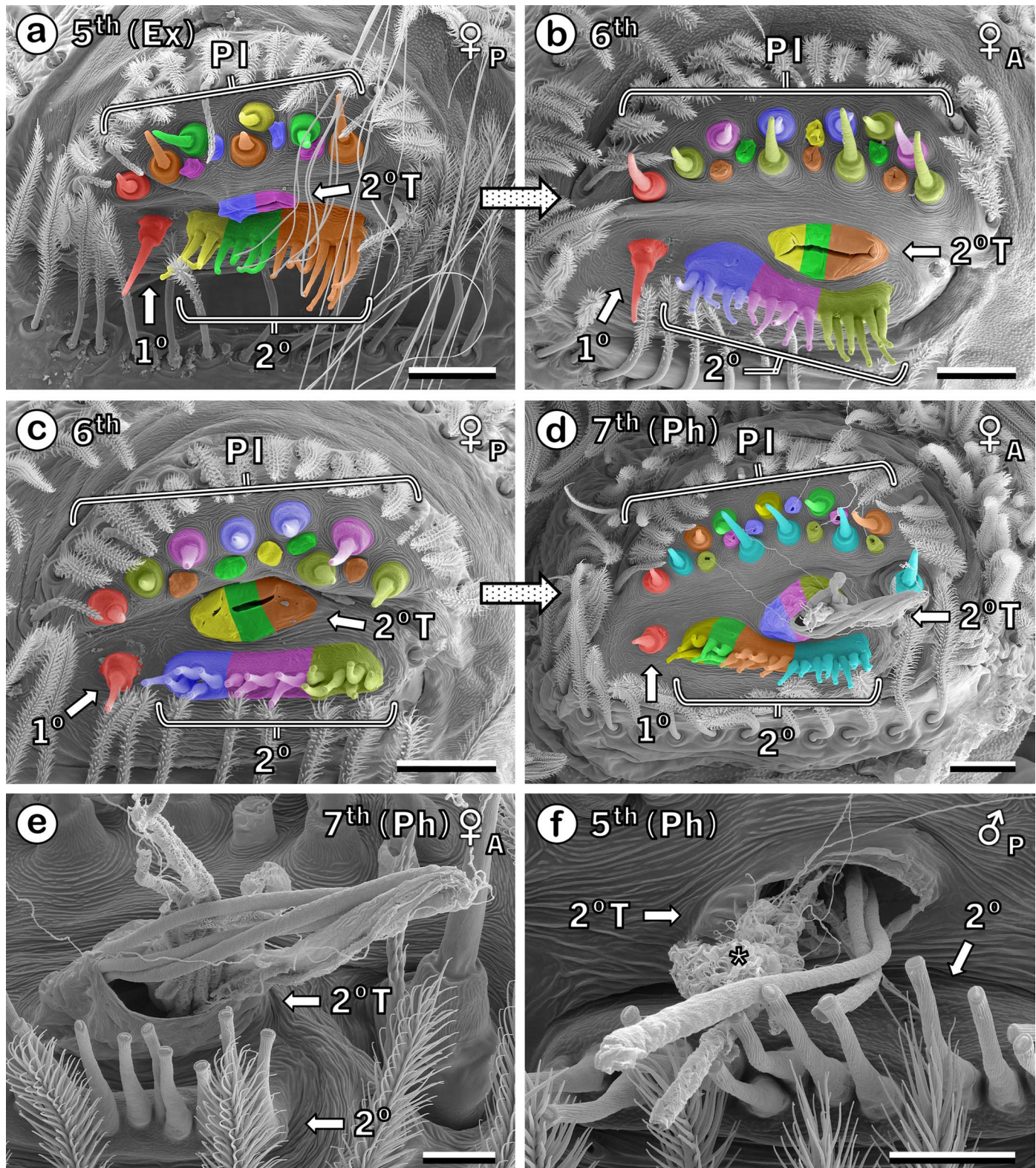


Figure 10.—Spinning fields on ALSs of *Palpimanus uncatus*. (a) Most recent exuvium shed by the adult female 6<sup>th</sup> instar shown in (b). Note silk fibers emerging from shafts of 2° MaA spigot on exuvium. (c, d) Female 6<sup>th</sup> (penultimate) instar well into proecdysis, showing the same spinning field on old (c) and new, pharate adult (d) exoskeletons. The most posterior PI spigot in (d) is set apart from the rest of the PI spinning field in a manner not observed in any other specimen and is a presumed minor abnormality. (e) Higher magnification and tilted view of 2° MaA tartipore (2° T) from (d). This tartipore was still accommodating 2° MaA ducts at the time of death. (f) A second example of a functioning 2° MaA tartipore in the newly formed exoskeleton of a pharate male 5<sup>th</sup> (penultimate) instar. Presumably as a result of enzymatic treatment used to remove soft tissues (see Methods), the 2° MaA (continued on next page)



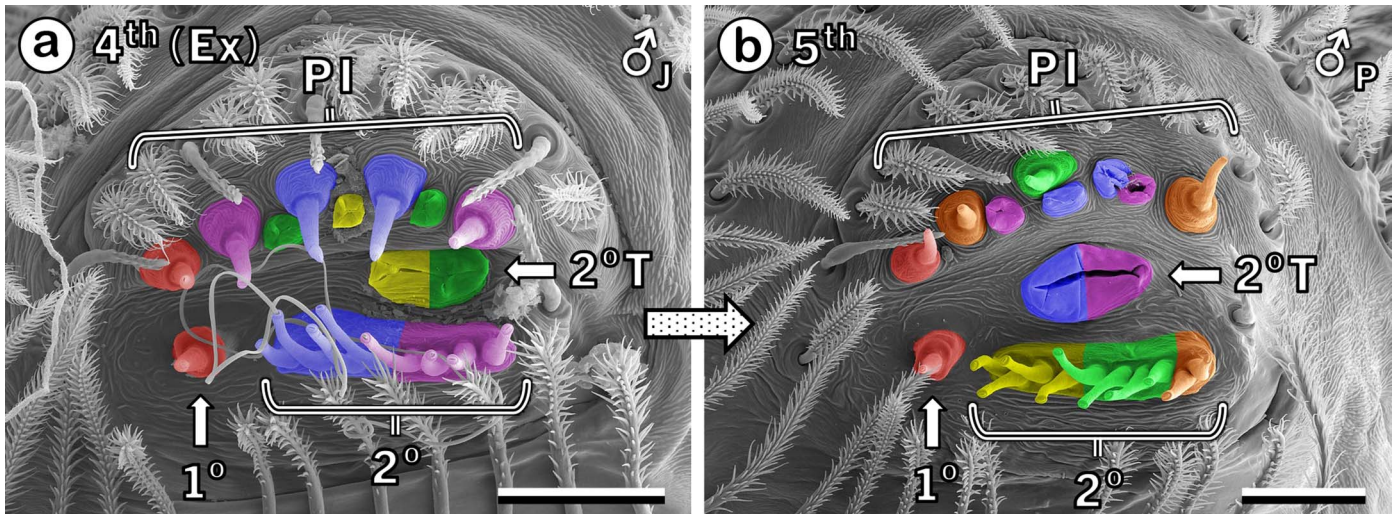


Figure 11.—Example of atypical PI ontogeny in *Palpimanus uncatus*, left ALS spinning fields. (a) Most recent exuvium shed by the male 5<sup>th</sup> (penultimate) instar shown in (b). The PI spigots and tartipores in (a) conform to the ‘standard pattern’, but those in (b) are missing two expected PI spigots that would have served T-A PIs last used during the 3<sup>rd</sup> stadium (see text). Specimen MCZ\_IJ\_163563. 1°, 1° MaA spigot; 2°, 2° MaA spigot; PI, PI spigots and tartipores; 2° T, 2° MaA tartipore. Scale bars = 20  $\mu$ m.

Murphy & Roberts 2015), and Stenochilidae (Murphy & Roberts 2015). Since there is no variation in the number of non-T-A PIs in *P. uncatus*, just as in the araneoids reported on thus far, ontogenetic increases in numbers of PI spigots that occur in these spiders and variation observed in PI spigot numbers within a stadium (Table 1) are the result of increases and variation in numbers of T-A PIs only.

In contrast, in four species from four genera of Lycosidae, only T-A PIs are present (Dolejš et al. 2014). These lycosids do, however, exhibit an analog to the PIs in *P. uncatus* with their ACs, a silk gland type absent in palpimanids. A single, medially-located non-T-A AC spigot is present on each PMS and PLS throughout all stadia and only the number of T-A AC spigots increases as the spider develops (Dolejš et al. 2014).

Thanks to the relatively small numbers of T-A PIs in *P. uncatus* and the linear arrangement of their spigots, a ‘standard pattern’ to the ontogenetic acquisition of new T-A PIs and PI spigots could be discerned in this spider. From a superficial perspective, this standard pattern presents simply as the numbers of T-A PI spigots and PI tartipores each increasing by one per ALS from one stadium to the next. But to fully appreciate the choreography that accompanies these increases, one should bear in mind that a T-A silk gland, in contrast to a non-T-A silk gland, is not used in every stadium after its formation, but only in every other stadium. For example, a T-A PI that develops toward the end of the 2<sup>nd</sup> stadium and is first used during the 3<sup>rd</sup> stadium will then not be used again until the 5<sup>th</sup> stadium. Thus, for T-A silk glands there exist within the opisthosoma an odd-stadia set and an even-stadia set of silk glands (see introductory comments and Terminology). So what initially looks like the addition of one PI and its spigot per ALS with each molt is actually achieved by the addition of two PIs and their spigots per ALS with each molt to either the

odd-stadia set or even-stadia set of T-A PIs in alternation. Where the two additional PI spigots form is not random. They take their places at opposite ends of a line of T-A PI structures (spigots and tartipores) representing earlier-formed T-A PIs and so extend this line at both ends. These standard pattern additions are shown in Figs. 8 and 9a–c, with color coding (Fig. 6) used to indicate the sequential additions of T-A PI spigots/tartipores and to reinforce that a given T-A PI, as represented by its spigot, is only used in alternate stadia, not every stadium.

The intrastadial variation seen in PI spigot and tartipore numbers in Table 1 demonstrates, however, that the standard pattern of increase in T-A PIs does not invariably occur, at least from the 4<sup>th</sup> stadium (and presumably from the 3<sup>rd</sup> given variation observed in PI tartipore numbers in female 4<sup>th</sup> instars). Upward and downward deviations from the standard pattern were seen in this study. Upward deviations were apparently normal parts of development, observed in females only, in which more than two T-A PIs were added to one of the sets of T-A PIs at one time. Downward deviations were seemingly minor developmental anomalies that afflicted both sexes, manifested as no change in number of T-A PI spigots from one stadium to the next, or even a decline.

Examples of upward deviations are shown in Fig. 10a–d where the number of PI spigots serving the newest members of a T-A PI set is three or more [this number happens to be three in 10a (brownish orange) and 10c (light green); five in 10b (light green) and 10d (turquoise)]. These deviations result in a sexual dimorphism whereby late stadium females have on average more T-A PI spigots than males and most if not all adult females have a larger number of T-A PI spigots than predicted by the standard pattern on at least one of their ALSs whereas few if any adult males do. Such a sexual dimorphism appears common among araneomorphs and is generally attributed to

FIGURE 10. (continued) ducts shown in (d–f) consist of just their cuticular linings, and even some of these appear to have been unravelled by the treatment. An especially distorted mass, seemingly composed of one or more cuticular linings, is indicated (\*). (a–e) Left ALS; (f) right ALS (image flipped horizontally). (a, b) Specimen MCZ\_IJ\_163564; (c–e) Specimen MCZ\_IJ\_163557; (f) Specimen UNHC\_0049459. 1°, 1° MaA spigot; 2°, 2° MaA spigot; PI, PI spigots and tartipores. Scale bars: (a–d) 25  $\mu$ m; (e, f) 10  $\mu$ m.



a shift in adult male priorities away from foraging and maintaining webs or retreats and toward seeking mates (Alfaro et al. 2018a). Other factors may emerge with further research. For example, if *P. uncatatus* females use PI silk during egg sac construction, directly or indirectly (no evidence for or against as yet), this might also contribute to maintaining the dimorphism.

The mechanism that produced 4 of 15 observed downward deviations from the standard pattern was not clear, but two mechanisms seemed to account for the other 11 deviations. By one of these, observed in 4 instances, only one new T-A PI was added to a T-A PI set at one time rather than the usual two. This was indicated by a T-A PI spigot added at only one end of the line of T-A PI spigots/tartipores rather than at both ends. By the other mechanism, accounting for the remaining 7 downward deviations, one or two T-A PIs that had been used in an earlier stadium did not return to service when expected (Fig. 11).

In examined araneoids, at least from the 2<sup>nd</sup> stadium, the location inferred for non-T-A PI spigots has consistently been at or close to the medial edge of the PI spinning field, roughly midway between its anterior and posterior ends (Fig. 9e) (Townley & Tillinghast 2009; Townley & Harms 2017). In *P. uncatatus*, the inferred position for the non-T-A PI spigot on each ALS was likewise consistent, but it was instead anterior to all T-A PI spigots and tartipores. This location does, however, place the non-T-A PI spigot lateral to the 1° MaA spigot, similar to their disposition in araneoids (Fig. 9e). Moreover, in *Araneus* and *Mimetus*, one of the two non-T-A PI spigots per ALS also appeared to start off at the anterior edge of the PI spinning field in 1<sup>st</sup> instars (Townley & Tillinghast 2009).

Among examined Lycosidae, as the number of T-A PIs increases during a spider's ontogeny the PI spigots serving the newest PIs tend to form at the periphery of the PI spinning field (Dolejš et al. 2014). The same tendency is observed among araneoids (Fig. 9e) (Townley & Harms 2017). The linear arrangement of PI spigots again leaves *P. uncatatus* both similar to and different from many other CY Spigot clade members. T-A PI spigots added peripherally to a clustered PI spinning field, as in many lycosids and araneoids, include some that expand the field anteriorly and posteriorly. In this respect, *P. uncatatus* is similar, with the spigots of newly-formed T-A PIs extending the PI spinning field anteriorly and posteriorly. But in a clustered arrangement, peripheral spigot additions also expand the PI field laterally. This is not so much in evidence in *P. uncatatus*, either because, as in typical males, the PI field does not deviate from a single-file linear arrangement (Fig. 9c), or because, as in typical late stadium females (Fig. 10b,d), even when larger numbers of added T-A PI spigots result in formation of a second row, most spigots serving the newest T-A PIs in two-row regions appear to be medial to spigots of earlier T-A PIs. This interpretation derives from the observation that when the same ALS apical segment is viewed on consecutive exoskeletons (e.g., Figs. 8c to 8d, 9a to 9b to 9c), PI tartipores generally occur medial to spigots that serve T-A PIs returning to service. This suggests that T-A PI spigots in the more medial row, some clearly medial to PI tartipores, serve the newly formed PIs.

**1° and 2° MaAs.**—Among the unusual aspects of the spinnerets of *P. uncatatus* (and *P. gibbulus*, see drawings in Machado 1944; Murphy & Roberts 2015) is a spigot on each ALS that has multiple shafts emerging from a single base. This spigot appears to be a modified homolog of the uni-shaft 2° MaA spigot present in most CY Spigot clade spiders. Evidence for this multi-shaft spigot being the 2° MaA spigot includes:

- (1) a location typical for a 2° MaA spigot: medial to the PI spigot/tartipore array and posterior to a spigot that, though diminutive for its subtype, appears to be the 1° MaA spigot.
- (2) a tartipore just lateral to the multi-shaft spigot, as expected next to a T-A 2° MaA spigot, that is of correspondingly large size, able to accommodate multiple ducts connecting to multiple shafts on the 2° MaA spigot.
- (3) silk fibers routinely observed emerging from several or even all shafts on the multi-shaft spigot on exuvia (Figs. 8a, 9a,b,d, 10a, 12b,c). Silk emerging from 2° MaA spigots on exuvia is often seen in other CY Spigot clade spiders (Fig. 9e,f; also Townley et al. 1991 [figs. 14, 15], 1993 [fig. 4], 2013 [fig. 1A]; Townley & Tillinghast 2003 [figs. 8, 10, 19, 20], 2009 [figs. 2I, 5A, 6A, 13C]) and indicates its use during ecdysis (Dolejš et al. 2014). On the examined *P. uncatatus* exuvia, no doubt some shafts were without silk fibers because of fiber losses incurred while preparing spinnerets for SEM. Other such instances presumably reflected autonomy among individual shafts with respect to initiation of fibers.
- (4) multiple silk gland ducts encircled by the single massive tartipore lateral to the multi-shaft spigot on pharate cuticles (Fig. 10d–f).
- (5) a distribution of putative mechanoreceptors (Gorb & Barth 1996) as expected relative to spigots identified as 1° and 2° MaA spigots. This distribution is comparable to that observed in other members of the CY Spigot clade (Ramírez 2014; Ramírez et al. 2014; Murphy & Roberts 2015; Alfaro et al. 2018a, b), especially araneoids (cf. Figs. 9f and 12e,f) (Townley & Tillinghast 2009; Townley et al. 2013).
- (6) a sclerite that encircles the spigots identified as 1° and 2° MaA spigots, as observed by light microscopy (Murphy & Roberts 2015, plate 239). This sclerite apparently delimits the MaA spinning field. As Murphy & Roberts (2015: 12) note, such a sclerite is not readily discernible in SEM scans.

This proposed 2° MaA spigot homology implies that the two 2° MaAs, one in the odd-stadia set, one in the even-stadia set, associated with each ALS in typical CY Spigot clade spiders (Townley et al. 1993; Řezáč et al. 2017) have become modified in the lineage of *P. uncatatus*, each transformed into multiple 2° MaAs with new glands added in sync with molt-intermolt cycles during a spider's ontogeny. This presumes that each 2° MaA spigot shaft serves a separate 2° MaA (not yet investigated), just as typical spigots and each shaft on a cribellum serve a separate silk gland (Kovoor 1977, 1987; Peters 1987).

Like the sexual dimorphism involving T-A PIs, the number of shafts on 2° MaA spigots was larger in late stadium females than males, increasing on average with each molt in females but decreasing with the molt to maturity in males (Table 1). This penultimate-to-adult downward trend in males does not, however, necessarily signal the degeneration of 2° MaAs as it might initially appear. This is because of the two alternating, odd-stadia and even-stadia sets of 2° MaAs. With four males I was able to compare spinnerets at antepenultimate and adult stadia (4<sup>th</sup> and 6<sup>th</sup> stadia, respectively, thus comparing within the even-stadia set of 2° MaAs). Though a small sample, they indicated that more often than not the number of glands in the even-stadia set of 2° MaAs either continues to increase by 1–2 glands per ALS (5 of 8 ALSs) or goes unchanged (2 of 8) between antepenultimate and adult stadia. On only one of eight ALSs was degeneration of a single gland indicated by one less shaft on the adult 2° MaA spigot compared to that on the antepenultimate. Thus, the

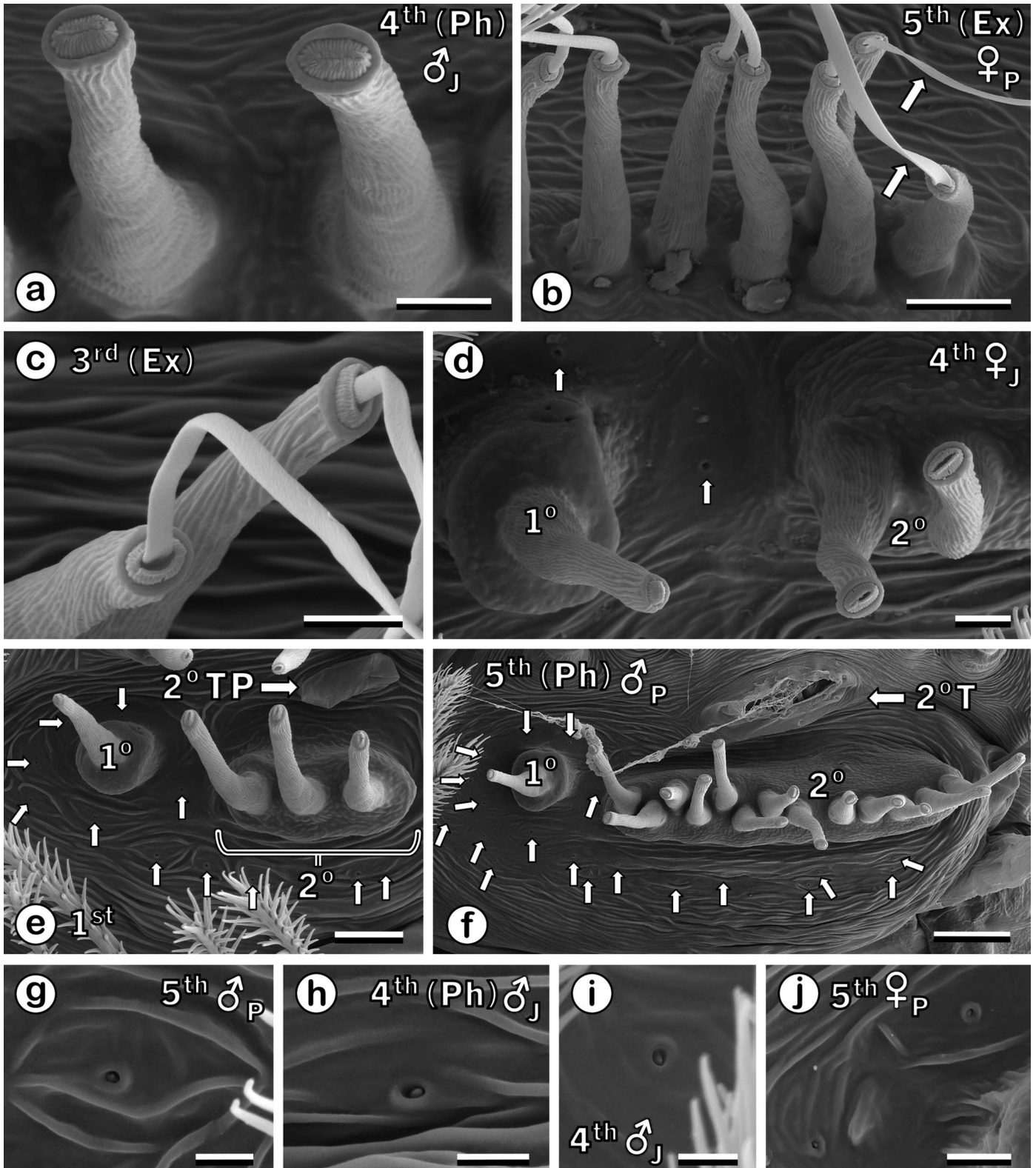


Figure 12.—Detailed views of MaA spinning field on ALSs in *Palpimanus uncatus*. (a) Distal ends of two  $2^{\circ}$  MaA spigot shafts with closed endpieces. (b–c)  $2^{\circ}$  MaA spigot shafts on exuvia with emerging silk fibers. Arrows in (b) point to especially ribbon-like fibers. (d) Distal ends of  $1^{\circ}$  versus  $2^{\circ}$  MaA spigot shafts. Arrows point to putative mechanoreceptors. (e–f) Distributions of mechanoreceptors (small unlabeled arrows) on MaA spinning field in a  $1^{\text{st}}$  instar (e) and pharate  $5^{\text{th}}$  instar (f). (g–j) Examples of mechanoreceptors showing raised-rim pores within thin regions of cuticle (Gorb & Barth 1996). A dendrite (D1 in Gorb & Barth 1996; Barth 2002) attachment site is visible at center of pores. (a–f, h) Left ALS; (g, i, j) right ALS (image flipped horizontally). (a, h) Specimen MCZ\_IJ\_163559; (b) Specimen UNHC\_0049463; (c) exuvium field-collected without spider; (d) Specimen UNHC\_0049451; (e) progeny of Specimen UNHC\_0049452, not deposited; (f) Specimen UNHC\_0049459; (g) Specimen MCZ\_IJ\_163563; (i) Specimen MCZ\_IJ\_163561; (j) Specimen MCZ\_IJ\_163562.  $1^{\circ}$ ,  $1^{\circ}$  MaA spigot;  $2^{\circ}$ ,  $2^{\circ}$  MaA spigot;  $2^{\circ}$  T,  $2^{\circ}$  MaA tartipore;  $2^{\circ}$  TP,  $2^{\circ}$  MaA tartipore primordium. Scale bars: (f) 10  $\mu\text{m}$ ; (b, e) 5  $\mu\text{m}$ ; (a, c, d, j) 2  $\mu\text{m}$ ; (g–i) 1  $\mu\text{m}$ .



sexual dimorphism in 2° MaA spigot shaft numbers appears to result less from 2° MaA degeneration in males and more from female increases, and also male increases within the odd-stadia set, outstripping male increases within the even-stadia set at the final molt.

Another demonstration of the importance of bearing in mind that T-A silk glands, like the 2° MaAs, occur as two different, alternately-functional sets of glands within the opisthosoma is shown in Fig. 8a,b, depicting right ALS spinning fields from one individual as they existed in the 1<sup>st</sup> and 2<sup>nd</sup> stadia. Note that 2° MaA spigot shafts numbered five and four, respectively, during these stadia. As with the penultimate-to-adult decline in males, this decrease by one shaft from one stadium to the next did not indicate the loss of a 2° MaA, only that a larger number of 2° MaAs composed the odd-stadia set than the even-stadia set during these early stadia in this particular individual.

Regarding the color coding of 2° MaA spigots in *P. uncatus* (Figs. 8–11), it is important to note that different colors applied to different groups of shafts on a single 2° MaA spigot, from two colors in 3<sup>rd</sup> (Fig. 8c) and 4<sup>th</sup> (Fig. 8d [pharate], 9a, 11a) instars up to four colors in a 7<sup>th</sup> instar (Fig. 10d [pharate]), are only intended to indicate that some of the 2° MaAs served by these shafts had been formed and used earlier—two, four, or six stadia earlier—and were returning to service, while other 2° MaAs had only recently developed and were functioning for the first time during the stadium indicated on the image. The number of shafts encompassed by one color is, in most instances, only an approximation based on mean numbers of shafts observed at different stadia (Table 1). In addition, I indicate that more anterior shafts on the 2° MaA spigot served 2° MaAs that formed earlier in the spider's ontogeny. For example, in Fig. 10d, shafts serving 2° MaAs that were first used by this individual when it was a 1<sup>st</sup> instar are colored yellow at the anterior end of the 2° MaA spigot. Posterior to these are shafts colored dark green serving 2° MaAs first used when the spider was a 3<sup>rd</sup> instar, followed by shafts colored brownish orange serving 2° MaAs first used when the spider was a 5<sup>th</sup> instar, and finally, at the posterior end of the spigot, shafts colored turquoise serving 2° MaAs that would have been used for the first time by the spider as a 7<sup>th</sup> instar. I depict shafts in this earlier-to-later-formed anterior-to-posterior sequence because the distance between the 1° MaA spigot and the anterior end of the 2° MaA spigot did not appear to change substantially from stadium to stadium as new shafts were added, creating the impression that new shafts were added at the posterior end of the 2° MaA spigot. But this is by no means certain. Indeed, other modes of shaft addition are entirely plausible, including the exact opposite (additions to the anterior end) or, reminiscent of T-A PI spigots, additions to both the anterior and posterior ends of the 2° MaA spigot simultaneously, especially if the non-T-A spigots (1° MaA, one PI, colored red in Figs. 7–11) shift anteriorly from one stadium to the next. Even if an anterior-to-posterior shaft addition trend is confirmed by further study, it may not be adhered to strictly. The same caveats apply to the color coding used on 2° MaA tartipores.

The 2° MaA spigots of *P. uncatus* are not the only multi-shaft spigots that have been observed among Araneomorphae. Oarcine Araneidae (Benavides et al. 2017) and some Symphytognathidae (Griswold et al. 1998) show a pair of AG spigot shafts emerging from a common base on PLSs, the former described as vestigial. Likewise, a pair of spigot shafts on a shared base occur on PMSs in species within Diguettidae, Plectreuridae, and Pholcidae (Platnick et al. 1991; Murphy & Roberts 2015). Though uncertainty remains, a MiA identity is indicated for this pair of shafts in Diguettidae,

while evidence, including histological observations (reviewed in Platnick et al. 1991), suggests a MiA+AC combination in Pholcidae, and either or both of these types remain plausible in Plectreuridae. Perhaps best known are multi-shaft paracribellar silk gland (PC) spigots on PMSs in juveniles and female adults belonging to some cribellate species within the families Stiphidiidae, Desidae, Dictynidae, and Austrochilidae (Peters 1983; Platnick et al. 1991; Griswold et al. 1999, 2005; Murphy & Roberts 2015). These spigots were brought to wider attention when the informal name 'Fused Paracribellar clade' was coined (Griswold et al. 1999) for a group composed of taxa currently assigned to Stiphidiidae and Desidae (Wheeler et al. 2017; World Spider Catalog 2024). This name suggests the multi-shaft PC spigots are the result of ancestral fusion of uni-shaft PC spigot bases, to which Murphy & Roberts (2015: 2) objected that fusion cannot be assumed. There are, however, multi-shaft spigots in which two shafts that clearly serve different silk gland types share the same base; specifically, one PC or AC-like spigot shaft and one PLS modified silk gland (MS) spigot shaft on a shared base, seen in some cribellates currently placed in Desidae, Amaurobiidae, and Zoropsidae (Griswold et al. 2005: figs. 87B,D, 88D; Ramírez 2014: fig. 135J; Murphy & Roberts 2015: Plates 30, 32[replacement page 227]). These especially seem best explained by spigot base fusion. Depictions of what might represent PC/MS spigot base fusions or secondary separations in progress have been presented for *Badumna* Thorell, 1890 (Desidae) (Murphy & Roberts 2015: plates 31, 33) and, likewise, partially conjoined multi- and uni-shaft PC spigot bases have been documented in *Pillara* Gray & Smith, 2004 (Stiphidiidae) (Griswold et al. 2005: fig. 71C). Fusions, not only of spigots, but of silk glands themselves have also been hypothesized in the evolution of ampullate silk glands and AGs (Kovoor 1987). The multi-shaft 2° MaA spigot of *P. uncatus*, on the other hand, appears to represent ancestral fission of a uni-shaft 2° MaA spigot and presumably this extends to fission of the 2° MaA served by the spigot, converting each single 2° MaA into multiple 2° MaAs. Interestingly, this conversion brought with it the capacity for ontogenetic increases in numbers of 2° MaAs (as indicated by increases in numbers of shafts) as is often observed with morphological multiples (Coddington 1989; Yu & Coddington 1990; Alfaro et al. 2018a). It is also notable, in relation to spigot base fusion and separation, that the 2° MaA spigot shown in Fig. 9b has one shaft (most posterior) that is actually on its own isolated base. This atypical arrangement presents an example of the variation natural selection can act upon in continually modifying the spinning apparatus.

The 2° MaA spigots of *P. uncatus* also recall spiders in the families Gradungulidae, Deinopidae, and Eresidae that have multiple T-A MaAs per ALS (Coddington 1989; Platnick et al. 1991; Peters 1992; Griswold et al. 2005; Miller et al. 2012). Those, however, are served by uni-shaft spigots and multiple tartipores, suggesting they evolved by a different mechanism from the one that resulted in the multi-shaft 2° MaA spigot and single 2° MaA tartipore of *P. uncatus*.

The elongated openings on the endpieces of the 2° MaA spigot shafts of *P. uncatus*, and the sometimes ribbon-like MaA fibers drawn from those endpieces (Fig. 12b, arrows), are also reminiscent of slit-opening MaA spigots and silk ribbons observed in the sicariid *Loxosceles* Heineken & Lowe, 1832 (Coddington et al. 2002; Knight & Vollrath 2002). However, the endpieces in *P. uncatus* seem to have greater flexibility than those of *Loxosceles*, their openings not necessarily restricted to narrow slits and thus with the ability to also draw fibers of rounder cross-section (Fig. 12b, left). In addition, though no measurements were made of fiber thicknesses in

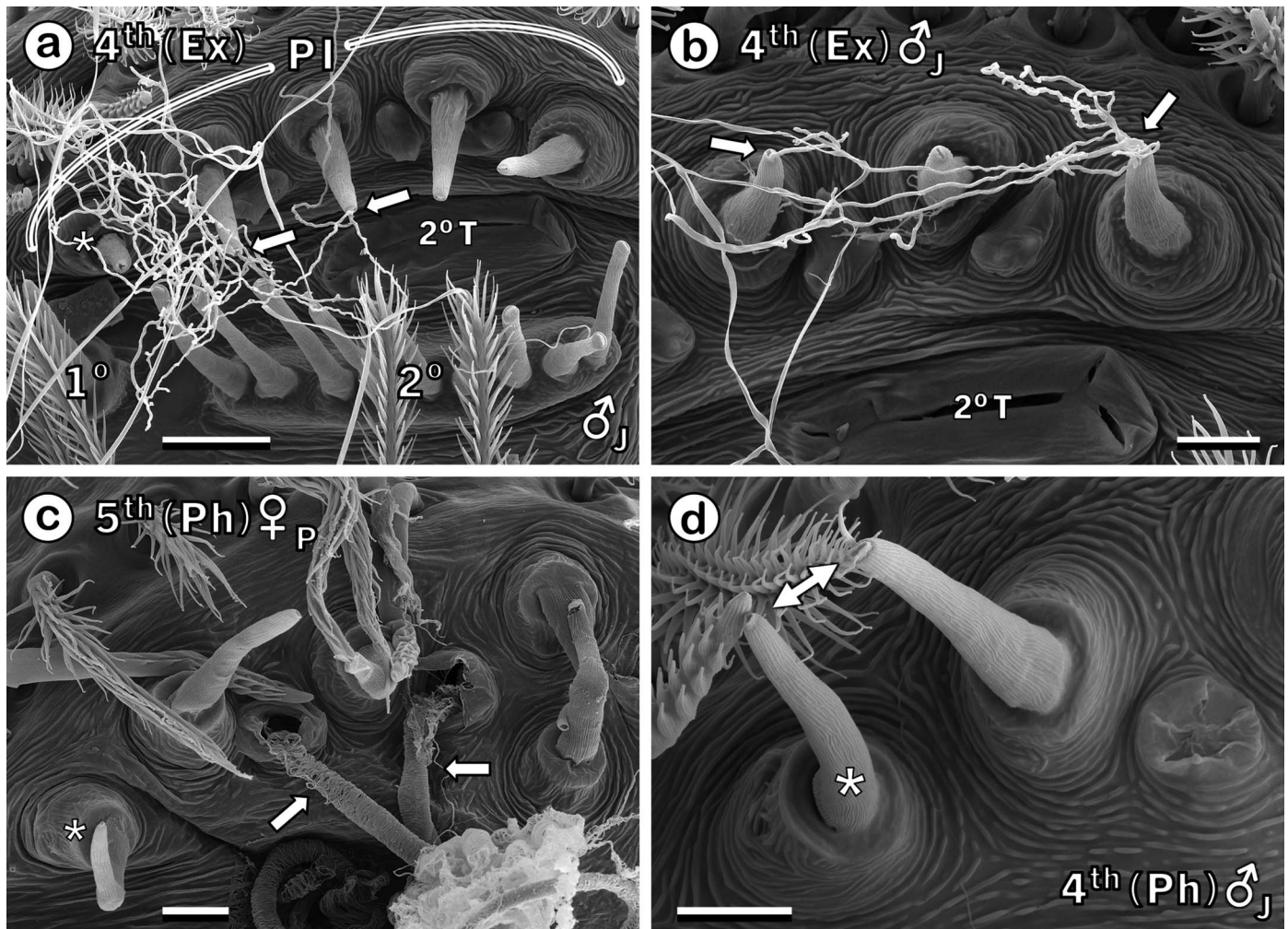


Figure 13.—Detailed views of PI spinning field on ALSs in *Palpimanus uncatus*. Non-T-A PI spigot indicated by asterisk (\*) in (a, c, d). All other PI spigots shown are T-A. (a–b) PI silk fibers emerging from spigots (arrows) on left (a) and right (b; image flipped horizontally) ALSs of one exuvium, showing PI silk use at ecdysis. (c) Functioning PI tartipores in the newly formed exoskeleton of a pharate female 5<sup>th</sup> (penultimate) instar. Two PI tartipores can be seen providing openings in the new exoskeleton, each allowing a single PI duct (arrows) to remain connected to PI spigots on the old exoskeleton through proecdysis and into ecdysis. Due to enzymatic removal of soft tissues (see Methods), ducts consist of cuticular linings only, partially unravelled by the treatment. (d) Comparison of non-T-A and T-A PI spigot endpieces (double-headed arrow). (c, d) Left ALS. (a, b) Specimen MCZ\_IJ\_163560; (c) Specimen UNHC\_0049451; (d) Specimen MCZ\_IJ\_163559. 1°, 1° MaA spigot; 2°, 2° MaA spigot; PI, PI spigots and tartipores; 2° T, 2° MaA tartipore. Scale bars: (a) 10 μm; (b–d) 5 μm.

this study, the extreme thinness of *Loxosceles* MaA silk (about 40–80 nm, Coddington et al. 2002; Knight & Vollrath 2002; Schniepp et al. 2013) does not appear to be matched by even those *P. uncatus* 2° MaA fibers that are ribbons.

**Functionality differences between T-A and non-T-A silk gland subtypes?**—For spiders that have both T-A and non-T-A subtypes of a silk gland type, one question we may ask is do they serve different functions? In some instances at least, the answer appears to be yes. For example, among some male mimetids, indications are that the two non-T-A PIs associated with each ALS become modified as maturity approaches, and their spigots in male adults display considerably enlarged openings relative to those of the T-A PI spigots (Townley & Tillinghast 2009; Townley et al. 2013; Benavides & Hormiga 2016). This suggests that the products of the non-T-A PIs differ from those of the T-A PIs and presumably play some role other than forming typical attachment discs. In *P. uncatus*, a difference in the diameters of the openings of non-T-A versus T-

A PI spigots was also noted, albeit much more subtle, and was the reverse of that seen in male adult mimetids, with openings on non-T-A PI spigots smaller than those on T-A PI spigots (Fig. 13d). It is unknown if this difference has any functional significance.

In one sense, however, T-A and non-T-A silk glands do exhibit a functional difference simply because the former can be used during proecdysis and the latter cannot. Indeed, for some silk glands, the T-A subtype may be used largely or only during proecdysis, as observed with 2° (T-A) MaAs in the araneid *Araneus cavaticus* (Keyserling, 1881) (Townley et al. 1993). Consequently, these 2° MaAs, presumably not involved in activities like orb web construction, would be under different selection pressures from the 1° (non-T-A) MaAs and their silks would thus be free to take on different physical properties. In *P. uncatus*, the functional difference between 1° and 2° MaAs during proecdysis was evident in the fact that exuvia had MaA fibers emerging only from 2° MaA spigots, never from 1° MaA spigots. Contrary to *A. cavaticus*, however, in *P. uncatus* it



seems very unlikely that use of the 2° MaA spigots, with their multiple shafts, is confined to proecdysis. Likewise, in spiders generally, use among T-A silk glands that occur as morphological multiples (PIs and ACs) is apparently not restricted to proecdysis.

**CYs, egg sacs, and maternal care.**—Because CY silk is used in the construction of egg sacs (Kovoor 1977; Ramírez 2014), a good indicator that certain spigots serve CYs—despite one described exception (Townley & Harms 2020)—is their presence on PMSs and PLSs of adult (and sometimes late juvenile) females and their absence in males (Coddington 1989). Though these spinneret types are degenerate in palpimanids (Jocqué & Dippenaar-Schoeman 2006; Platnick 2020), spigots that meet this condition (Table 1; cf. Fig. 5c,d) occur on the PS in all three palpimanid subfamilies (Platnick et al. 1999; Zonstein & Marusik 2013, 2017; Murphy & Roberts 2015) and were identified as CY spigots by Murphy & Roberts (2015).

Among female adults of *P. uncatus* in this study, the number of CY spigots on the PS ranged from 33–44 (Table 1). In adult *P. gibbulus*, 36 CY spigots are shown in Machado's (1944) fig. 13 whereas 60 CY spigots are indicated in Murphy & Roberts' (2015) plate 239 given that half the PS (showing 30 CY spigots) is apparently depicted. This agrees with their family definition of Palpimanidae in which they report that, among its members, the PMS and PLS portions of half the PS contain about 2–25 and 3–6 CY spigots, respectively, for an approximate range in the family, over the entire PS, of 10–62 CY spigots. Though the limits of the PMS and PLS portions of the PS were not apparent by SEM in this study (Figs. 5d, 15c), plate 239 in Murphy & Roberts (2015) indicates that a subtle border between them may be discerned by light microscopy. The chedimine *B. pumilus*, shown in plate 238 of the same work, was apparently the basis for the low end of the family range, with about 10 CY spigots indicated over the entire PS. In the otiothopine *O. pentucus*, about 16 CY spigots on the PS are indicated in fig. 257 in Platnick et al. (1991) which appears to show eight spigots on half the PS.

While not unprecedented, the numbers of CY spigots in *Palpimanus* exceed those in many CY Spigot clade members (Kovoor 1977, 1987). Machado (1944) hypothesized that this impressive battery of spigots evolved after the reduction of the OS5 spinnerets (PLS + PMS). If their identification as CY spigots is correct, it would not come as a surprise for these spiders to produce substantial egg sacs. Though information on maternal care in Palpimanidae, including egg sac construction, is very limited (Guo et al. 2021), photographs of the egg sac of *Palpimanus paroculus* Simon, 1910 have recently been published (Dippenaar-Schoeman et al. 2020). In addition, Leroy & Leroy (2000: 83) presented a photo of a female palpimanid from southern Africa, much of her egg sac, and, very close to their mother (a few possibly in contact), several spiderlings. These were identified as an *Iheringia* sp. Keyserling, 1891, currently synonymized (Platnick 1975; World Spider Catalog 2024), suggesting a *Diaphorocellus* sp. Simon, 1893 identity. However, the mother lacks the dorsal abdominal patterning seen in *Diaphorocellus*, two-colored or finely spotted (Zonstein & Marusik 2020), and appears instead to be a *Palpimanus* sp. (see Dippenaar-Schoeman et al. 2020). These egg sacs appear similar to those of *P. uncatus* observed during this study (Fig. 2a,b)—rotund overall, though seemingly at least somewhat flattened on the bottom, with a dense cover of white silk (less dense on the flattened end, at least in *P. uncatus*). The point at the top of the egg sac of *P. uncatus* can also be clearly seen on the egg sac of *P. paroculus* (Dippenaar-Schoeman et al. 2020). All these egg sacs qualify as substantial and thus support a CY spigot identity. It should be noted, however, that

no investigation has been made of the silk composing the egg sac to verify its origin or determine if it contains more than one type of silk. Construction of an egg sac was not observed during this study, but the finished product could be readily transported by the mother, held in her chelicerae (Fig. 2a), and was guarded by her, though she could still capture and feed on prey while on guard. Egg sac and spiderling guarding are also indicated in other *Palpimanus* species (Leroy & Leroy 2000; Dippenaar-Schoeman & Haddad 2014; Dippenaar-Schoeman et al. 2020). Spiderlings (1<sup>st</sup> instars) of *P. uncatus* emerged from two egg sacs built in the greenhouse through a large opening that seemed to have been created by the mother. Even if true, it remains to be determined if mothers open egg sacs for young under natural conditions or if these instances were due to the unnatural and less-than-ideal conditions in the greenhouse.

The number of eggs deposited in the field-made egg sac, which had no openings until I opened it, was 38. Three egg sacs made in the laboratory must have contained at least 9–15 eggs each upon completion, but each of these egg sacs had already been opened before I surveyed their contents and there were indications that females sometimes fed on their own eggs. Thus, the one field datum is currently the most reliable indicator of fecundity in *P. uncatus*. Egg sacs of *Palpimanus potteri* Lawrence, 1937 have yielded 45 and 9 spiderlings, and 13 emerged from an egg sac of *P. gibbulus* (Pekár & Líznavá 2023).

In *P. gibbulus*, Machado (1944) observed that the first spigots to form on the PS in female juveniles were located at the lateral ends of the PS, within the region ancestrally occupied by PLSs. In this study, CY spigots were first noted in female 4<sup>th</sup> instars and in one such individual that had only two CY spigots, one of these was positioned about midway on the left half of the PS, the other was even more medially placed (i.e., in a presumed ancestral PMS position) on the right half of the PS. In two 4<sup>th</sup> instars with six CY spigots, these were either roughly evenly spaced over the PS (Fig. 15a) or more congregated about midway on each half of the PS (Fig. 14f). An ontogenetic trend was noted, however, for CY spigots to be added in a lateral-to-medial progression once the number of spigots required more than one row. Descriptions in Machado (1944) also suggest that, in *P. gibbulus*, CY spigots potentially first appear in female 3<sup>rd</sup> instars. However, more female juveniles of both species need to be examined to confirm or invalidate this species difference.

**Prey.**—When I began maintaining *P. uncatus* in the greenhouse in 2014, I was hesitant to attempt using jumping spiders (Salticidae) as prey, fearing their visual acuity would give them a predatory advantage. Had I been familiar with the study of Cerveira & Jackson (2005), I would have felt differently. They describe in detail frequent predation by a Ugandan *Palpimanus* sp. on salticids. Likewise, knowledge of the results contained in Pekár et al. (2011b) would have altered my approach since they observed >90% capture success by *P. gibbulus* and *Palpimanus orientalis* Kulczyński, 1909 in encounters with a salticid species that is itself araneophagic. Ignorant of those studies, and starting cautiously with small salticids, I gradually formed an anecdotal impression that salticids make very suitable prey for *P. uncatus*, so much so as to increasingly make the family a focus of our collecting excursions for prey. Analysis of palpimanid gut contents has confirmed a high incidence of predation on salticids by *P. potteri* and *P. gibbulus* and has indicated that, in general, a large majority of a palpimanid's diet is made up of cursorial spiders, living in the same microhabitat, that hide in retreats (Pekár et al. 2022). Nevertheless, *Palpimanus* also prey on a variety of web-building spiders (Pekár et al. 2011b, 2022). This agrees with observations made during this

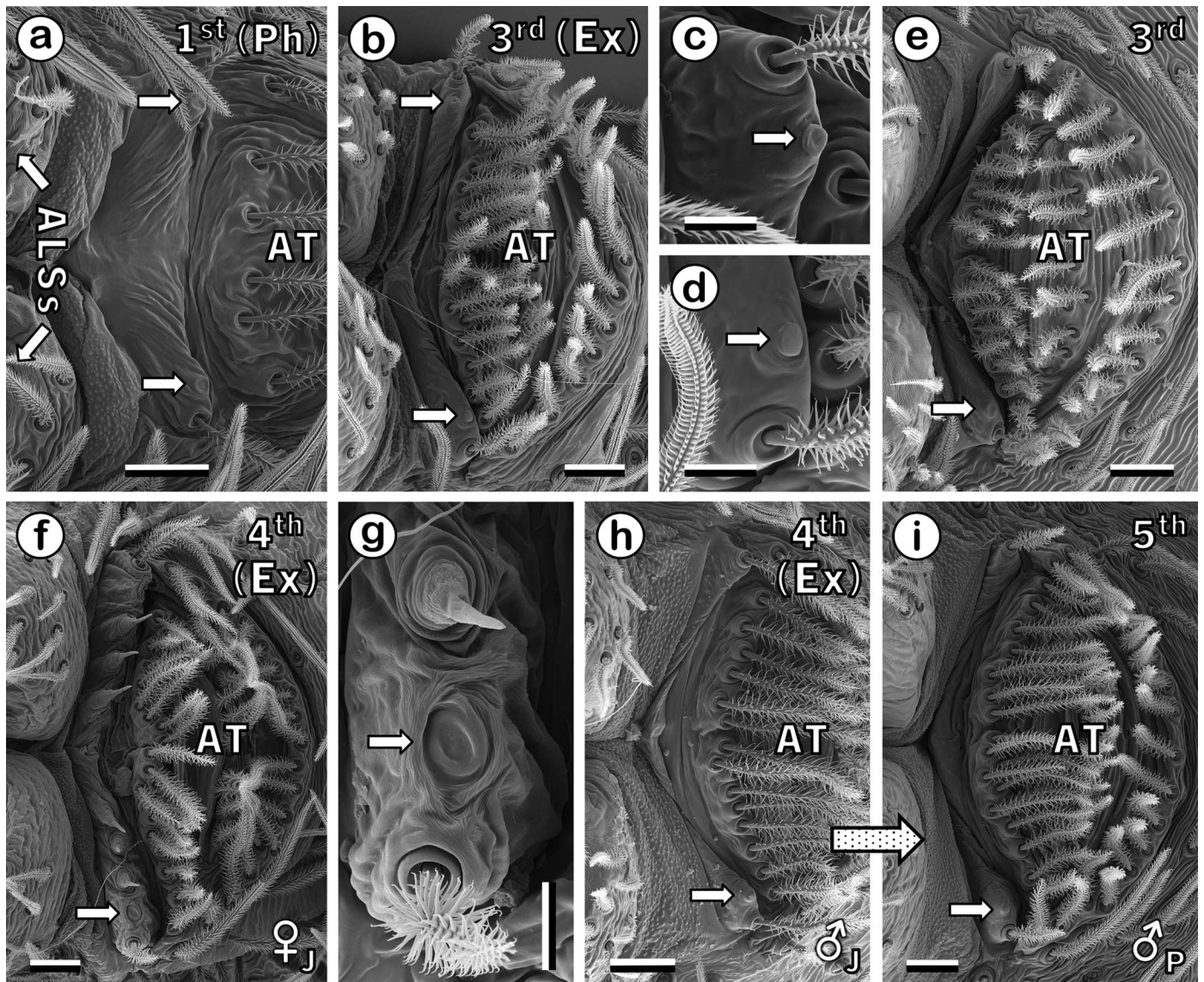


Figure 14.—Examples of the PS at four stadia in juvenile *Palpimanus uncatus*. Posterior portions of ALSs at left in (a, b, e, f, h, i), as labeled in (a). Small unlabeled arrows point to circular structures (disks) of unknown nature and function observed at one (e, f, h, i) or both (a, b) ends of the PS in many individuals. Those in (b) and (f) shown at higher magnification in (c, d) and (g), respectively. Spigots in (f, g) presumed to be CY spigots. (a) Specimen UNHC\_0049454; (b–d) exuvium field-collected without spider; (e) Specimen UNHC\_0049461; (f, g) Specimen UNHC\_0049460; (h, i) Specimen MCZ\_IZ\_163563. AT, anal tubercle. Scale bars: (a, b, e, f, h, i) 25  $\mu\text{m}$ ; (c, d, g) 10  $\mu\text{m}$ .

study, with spiders from 16 families, cursorial and web-building, successfully preyed upon by *P. uncatus*. Representatives of 13 of these families were also predated by *Palpimanus* in Pekár et al. (2011b), with only Pholcidae, Pisauridae, and Uloboridae not represented in their table 1, though the pholcid *Pholcus* Walckenaer, 1805 has previously been used to feed *P. gibbulus* in the laboratory (Uhl & Schmitt 1996).

Among four species of Palpimanidae, including representatives of all three subfamilies and two species of *Palpimanus*, gut content DNA analysis did not reveal significant differences in diet composition among male and female adults and juveniles, indicating that prey composition does not shift substantially with ontogeny (Pekár et al. 2022). This again agrees with observations made during this study, including on five 1<sup>st</sup> instars of *P. uncatus* in which an araneophagic inclination was already evident, with members of four spider

families, cursorial and web-building, preyed upon (the only early stadia prey on hand at the time). These four families were among the 16 families predated by later instars.

The average time between successful feedings in this study, about 13 days, is close to the 14 days obtained for *P. orientalis* and longer than observed for more euryphagic spiders (Pompozzi et al. 2019). Among other factors, this difference between specialists like *Palpimanus* and generalists may arise from the ability of specialists to subdue larger prey on average and use them more efficiently (Pompozzi et al. 2019) and from a lower metabolic rate in *Palpimanus* (Pekár et al. 2022; Pekár & Líznarová 2023).

Attempts were made to obtain additional viable egg sacs by housing female and male adults in the same box. Though no egg sacs resulted, it was of interest that no sexual cannibalism occurred



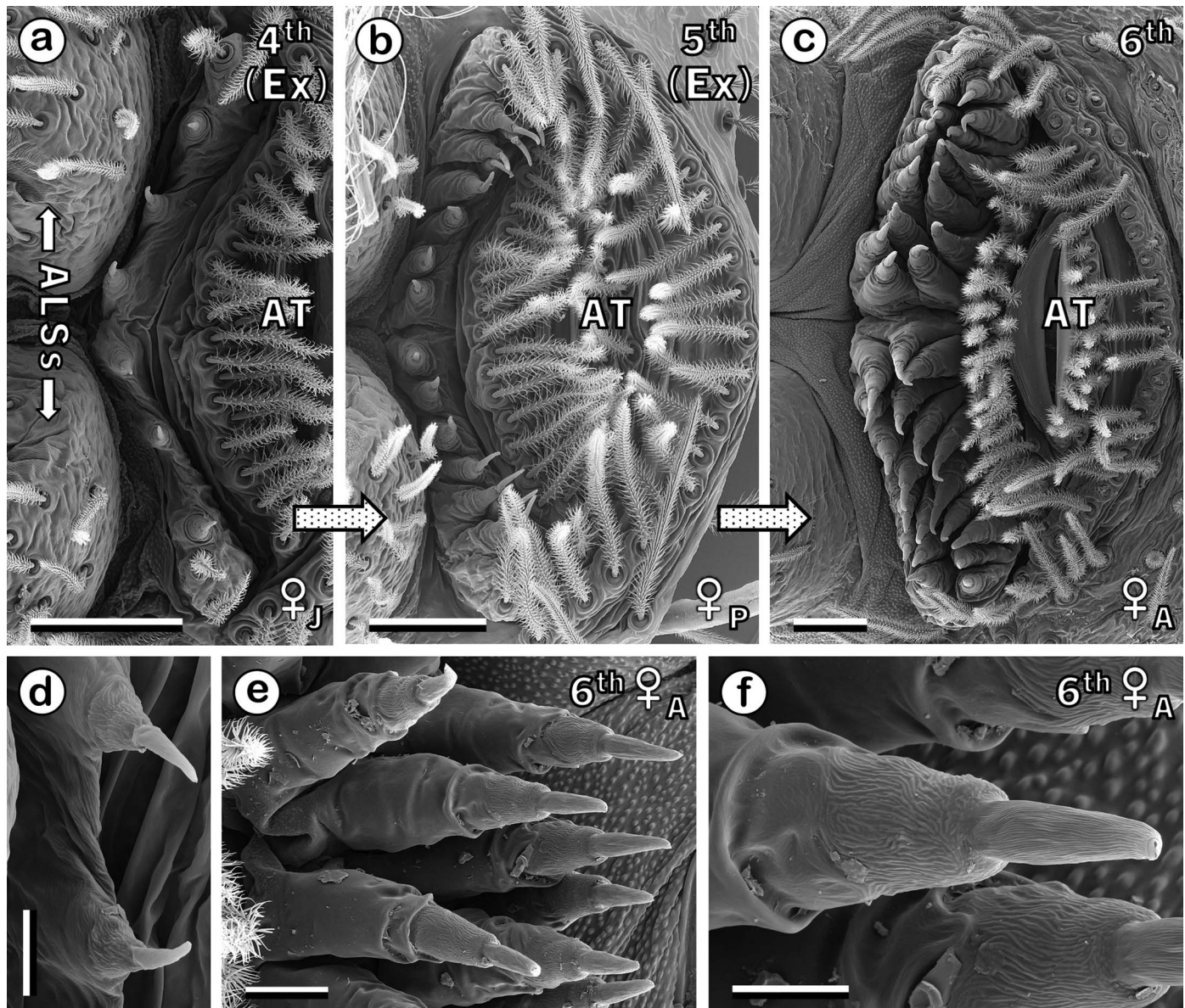


Figure 15.—PS in female *Palpimanus uncatus*. All spigots presumed to be CY spigots. (a, b) Two most recent exuvia shed by the adult 6<sup>th</sup> instar shown in (c). Posterior portions of ALSs at left in (a–c), as labeled in (a). (d) Higher magnification, anterior view of two CY spigots from right central PS in (a). (e) Detail of CY spigots from another adult 6<sup>th</sup> instar. Note the cuticular silo supporting each spigot. (f) Detail of central CY spigot from (e). (a–d) Specimen UNHC\_0049463; (e, f) Specimen UNHC\_0049456. AT, anal tubercle. Scale bars: (a–c) 50  $\mu$ m; (e) 20  $\mu$ m; (d, f) 10  $\mu$ m.

despite adult pairs cohabiting for between 4 and 73 days and despite each adult being paired at different times with multiple potential mates. This agrees with earlier observations in *P. orientalis* and *P. gibbulus* in which the incidence of cannibalism in laboratory trials increased with increasing difference in prosomal size between interacting conspecifics and occurred only when a > 2-fold difference existed between the pair (Líznařová et al. 2018). *Palpimanus* stridulate as part of their defensive strategy and to communicate with conspecifics (Uhl & Schmitt 1996; Dippenaar-Schoeman & van den Berg 2010; Uhl & Elias 2011; Dippenaar-Schoeman et al. 2013; Pekár et al. 2020) and there is evidence that stridulation is especially important in reducing predation on small juvenile *Palpimanus* by larger conspecifics, but it may also inhibit sexual cannibalism (Líznařová et al. 2018). Counter to observations of a low incidence of

cannibalism in *Palpimanus*, gut content DNA analysis has indicated frequent cannibalism in two species of *Palpimanus* (Pekár et al. 2022). These authors, however, advise caution, citing mitochondrial heteroplasmy (> 1 mitochondrial genotype in an individual) and sequencing errors as factors that may have inflated the estimated frequency of cannibalism.

**Molts to maturity and longevity.**—Pekár & Líznarová (2023) obtained 1<sup>st</sup> to 5<sup>th</sup> stadium juveniles, though no adults, when they raised *Palpimanus* of three species from egg sacs. This is consistent with results from this study in which all adults (5 ♂, 8 ♀) were estimated to have been in their 6<sup>th</sup> stadium. However, one female that died as a penultimate instar during proecdysis was also estimated to have been in her 6<sup>th</sup> stadium (Table 1). Nevertheless, 6<sup>th</sup> stadium adults of both sexes seem to be typical among *Palpimanus*.



Citing unpublished data, Líznavá et al. (2018) reported that *Palpimanus* have a lifespan of up to three years which agrees with observations made on female *P. uncatus* during this study. For male *P. uncatus*, evidence suggested a potential two-year lifespan. After raising three species of *Palpimanus* from egg sacs for more than a year, Pekár & Líznavá (2023) also concluded that *Palpimanus* have a life cycle that is at least biennial.

#### ACKNOWLEDGMENTS

This paper is dedicated to the memory of Professor Edward K. Tillinghast (1932–2021); mentor, role model, colleague, and dear friend to so many.

It is with pleasure and gratitude that I acknowledge the incalculable debt I owe Mike Taylor and Anna Stamatiou (chiosnature.org) for encouraging and greatly facilitating the collecting trip to Chios. Mike provided extensive logistical support in preparation for the trip and warm hospitality on the island. Anna made her translation skills freely available, making the process of requesting permission to export live spiders far easier than it would have been otherwise. Sincere thanks to the Specialized Forestry Service, Department C of the Ministry of the Environment, Energy, and Climate Change of Greece (Dimitrios Germanos, Head of Directorate of Environmental Planning) for this permission (Permit no. 104696/161; 12 Feb 2014) and to the US Fish & Wildlife Service for permission to import the spiders (Cleared USFWS 22 May 2014). I am also grateful to my favorite traveling and spider collecting companions, Charlene D. Newton and Lindsay M. Newton, for their critical contributions to collecting specimens, including the field-collected egg sac of *P. uncatus* (LMN), to Pat Watts and Scott Gasperin for photographing live spiders, and to István Mikó (UNHC) and Adam J. Baldinger (MCZ) for depositing specimens in the collections they curate. CD Newton also helped collect spider prey for *P. uncatus*. Many thanks also to Martín J. Ramírez and an anonymous reviewer for their many helpful suggestions that greatly improved this report. The Tescan SEM so essential to this study was purchased with funds from the US National Science Foundation (MRI Grant 1337897) with additional funds from UNH. The Nikon CLSM used was purchased by UNH's Center for Integrated Biomedical and Bioengineering Research (CIBBR) through a grant from the National Institute of General Medical Sciences of the US National Institutes of Health (Grant P20GM113131). A staff professional development grant from UNH helped defray travel expenses.

#### SUPPLEMENTAL MATERIALS

Supplemental Appendix 1.—Detailed location information for *Palpimanus uncatus* collected on the island of Chios (Χίος, Khíos), Greece, online at <https://doi.org/10.1636/JoA-S-22-056.s1>

#### LITERATURE CITED

- Alfaro RE, Griswold CE, Miller KB. 2018a. Comparative spigot ontogeny across the spider tree of life. *PeerJ* 6:e4233. doi: 10.7717/peerj.4233
- Alfaro RE, Griswold CE, Miller KB. 2018b. The ontogeny of the spinning apparatus of *Tengella perfuga* (Araneae: Zoropsidae). *Invertebrate Biology* 137:187–204. doi: 10.1111/ivb.12219
- Ayoub NA, Friend K, Clarke T, Baker R, Correa-Garhwal SM, Crean A, et al. 2021. Protein composition and associated material properties of cobweb spiders' gumfoot glue droplets. *Integrative and Comparative Biology* 61:1459–1480. doi: 10.1093/icb/icab086
- Barth FG. 2002. *A Spider's World: Senses and Behavior*. (A Biederman-Thorson, transl.). Springer-Verlag, Berlin.
- Benavides LR, Hormiga G. 2016. Taxonomic revision of the Neotropical pirate spiders of the genus *Gelanor* Thorell, 1869 (Araneae, Mimetidae) with the description of five new species. *Zootaxa* 4064:1–72. doi: 10.11646/zootaxa.4064.1.1
- Benavides LR, Giribet G, Hormiga G. 2017. Molecular phylogenetic analysis of “pirate spiders” (Araneae, Mimetidae) with the description of a new African genus and the first report of maternal care in the family. *Cladistics* 33:375–405. doi: 10.1111/cla.12174
- Blackledge TA, Kuntner M, Agnarsson I. 2011. The form and function of spider orb webs: Evolution from silk to ecosystems. *Advances in Insect Physiology* 41:175–262. doi: 10.1016/B978-0-12-415919-8.00004-5
- Bosmans R, Baert L, Bosselaers J, De Koninck H, Maelfait J-P, Van Keer J. 2009. Spiders of Lesbos (Greece): A catalogue with all currently known spider reports from the Eastern Aegean Island of Lesbos. *Newsletter of the Belgian Arachnological Society, Arachnological Contributions* 24(suppl.):1–72. [belgianspiders.be/wp-content/uploads/2018/12/Bosmans\\_et\\_al.\\_2009\\_Nie\\_24\\_1-70-Lesbos.pdf](http://belgianspiders.be/wp-content/uploads/2018/12/Bosmans_et_al._2009_Nie_24_1-70-Lesbos.pdf)
- Cala-Riquelme F, Quijano-Cuervo L, Sabogal-González A, Agnarsson I. 2018. New species of Otiotopinae (Araneae: Palpimanidae) from Colombia. *Zootaxa* 4442:413–426. doi: 10.11646/zootaxa.4442.3.4. Erratum: *Zootaxa* 4459:600. doi: 10.11646/zootaxa.4459.3.12
- Cerveira AM, Jackson RR. 2005. Specialised predation by *Palpimanus* sp. (Araneae: Palpimanidae) on jumping spiders (Araneae: Salticidae). *Journal of East African Natural History* 94:303–317. doi: 10.2982/0012-8317(2005)94[303:SPBPSA]2.0.CO;2
- Chaw RC, Hayashi CY. 2018. Dissection of silk glands in the Western black widow *Latrodectus hesperus*. *Journal of Arachnology* 46:159–161. doi: 10.1636/JoA-16-S-063.1
- Clarke TH, Garb JE, Haney RA, Chaw RC, Hayashi CY, Ayoub NA. 2017. Evolutionary shifts in gene expression decoupled from gene duplication across functionally distinct spider silk glands. *Scientific Reports* 7:8393. doi: 10.1038/s41598-017-07388-1
- Coddington J. 1983. A temporary slide mount allowing precise manipulation of small structures. *Verhandlungen des Naturwissenschaftlichen Vereins in Hamburg* (NF) 26:291–292.
- Coddington JA. 1989. Spinneret silk spigot morphology: evidence for the monophyly of orbweaving spiders, Cyrtophorinae (Araneidae), and the group Theridiidae plus Nesticidae. *Journal of Arachnology* 17:71–95. [www.jstor.org/stable/3705406](http://www.jstor.org/stable/3705406)
- Coddington JA, Chanzy HD, Jackson CL, Raty G, Gardner KCH. 2002. The unique ribbon morphology of the major ampullate silk of spiders from the genus *Loxosceles* (recluse spiders). *Biomacromolecules* 3:5–8. doi: 10.1021/bm010108m
- Dippenaar-Schoeman AS, Haddad CR. 2014. Spiders of the Grassland Biome (Plant Protection Research Institute Handbook No. 19). Agricultural Research Council-PPRI, Pretoria.
- Dippenaar-Schoeman AS, Jocqué R. 1997. African Spiders: An Identification Manual (Plant Protection Research Institute Handbook No. 9). Biosystematics Division, Agricultural Research Council-PPRI, Pretoria.
- Dippenaar-Schoeman AS, van den Berg AM. 2010. Spiders of the Kalahari (Plant Protection Research Institute Handbook No. 18). Agricultural Research Council-PPRI, Pretoria
- Dippenaar-Schoeman AS, Foord SH, Haddad CR. 2013. Spiders of the Savanna Biome. University of Venda, Thohoyandou & Agricultural Research Council, Pretoria.
- Dippenaar-Schoeman AS, Haddad CR, Foord SH, Lotz LN. 2020. South African National Survey of Arachnida Photo Identification Guide: The Palpimanidae of South Africa. 2020 version 1:1–25. doi:10.5281/zenodo.6813794
- Dolejš P, Buchar J, Kubcová L, Smrž J. 2014. Developmental changes in the spinning apparatus over the life cycle of wolf spiders (Araneae: Lycosidae). *Invertebrate Biology* 133:281–297. doi: 10.1111/ivb.12055



- Downen MR, Selden PA. 2021. The earliest palpimanid spider (Araneae: Palpimanidae), from the Crato Fossil-Lagerstätte (Cretaceous, Brazil). *Journal of Arachnology* 49:91–97. doi: 10.1636/JoA-S-19-059
- Downes MF. 1987. A proposal for standardization of the terms used to describe the early development of spiders, based on a study of *Theridion rufipes* Lucas (Araneae: Theridiidae). *Bulletin of the British Arachnological Society* 7:187–193. [www.britishtspiders.org.uk/system/files/library/070609.pdf](http://www.britishtspiders.org.uk/system/files/library/070609.pdf)
- Forster RR, Platnick NI. 1984. A review of the archaeid spiders and their relatives, with notes on the limits of the superfamily Palpimanoidea (Arachnida, Araneae). *Bulletin of the American Museum of Natural History* 178:1–106. [hdl.handle.net/2246/991](http://hdl.handle.net/2246/991)
- Gorb SN, Barth FG. 1996. A new mechanosensory organ on the anterior spinnerets of the spider *Cupiennius salei* (Araneae, Ctenidae). *Zoomorphology* 116:7–14. doi: 10.1007/BF02526925
- Griswold CE, Coddington JA, Hormiga G, Scharff N. 1998. Phylogeny of the orb-web building spiders (Araneae, Orbiculariae: Deinopoidea, Araneioidea). *Zoological Journal of the Linnean Society* 123:1–99. doi: 10.1111/j.1096-3642.1998.tb01290.x
- Griswold CE, Coddington JA, Platnick NI, Forster RR. 1999. Towards a phylogeny of entelegyne spiders (Araneae, Araneomorphae, Entelegynae). *Journal of Arachnology* 27:53–63. [www.jstor.org/stable/3705965](http://www.jstor.org/stable/3705965)
- Griswold CE, Ramírez MJ, Coddington JA, Platnick NI. 2005. Atlas of phylogenetic data for entelegyne spiders (Araneae: Araneomorphae: Entelegynae) with comments on their phylogeny. *Proceedings of the California Academy of Sciences, 4<sup>th</sup> Series* 56(Supplement II):1–324. [repository.si.edu/handle/10088/14866](http://repository.si.edu/handle/10088/14866)
- Guo X, Selden PA, Ren D. 2021. Maternal care in Mid-Cretaceous lagonomegopid spiders. *Proceedings of the Royal Society B* 288:20211279. doi: 10.1098/rspb.2021.1279
- Heath D. 1995. *An Introduction to Experimental Design and Statistics for Biology*. UCL Press, London.
- Hernández-Corral J, Ferrández MA. 2017. Descripción de una especie nueva de *Palpimanus* Dufour, 1820 de Marruecos (Araneae: Palpimanidae), con notas sobre los *Palpimanus* del Mediterráneo. *Revista Ibérica de Aracnología* 30:37–46.
- Hilbrant M, Damen WGM. 2015. The embryonic origin of the ampullate silk glands of the spider *Cupiennius salei*. *Arthropod Structure & Development* 44:280–288. doi: 10.1016/j.asd.2015.04.001
- Jocqué R, Dippenaar-Schoeman AS. 2006. *Spider Families of the World*. Royal Museum for Central Africa, Tervuren.
- Knight DP, Vollrath F. 2002. Spinning an elastic ribbon of spider silk. *Philosophical Transactions of the Royal Society of London, Series B* 357:219–227. doi: 10.1098/rstb.2001.1026
- Kovoor J. 1972. Étude histochemique et cytologique des glandes séricigènes de quelques Argiopidae. *Annales des Sciences Naturelles, Zoologie et Biologie Animale, 12<sup>e</sup> Série* 14:1–40.
- Kovoor J. 1977. La soie et les glandes séricigènes des arachnides. *L'Année Biologique, 4<sup>e</sup> Série* 16:97–171.
- Kovoor J. 1984. Anatomie, histologie et affinités de l'appareil séricigène des *Hersilia* Sav. et Aud. (Araneae: Hersiliidae). *Canadian Journal of Zoology* 62:97–106. doi: 10.1139/z84-017
- Kovoor J. 1987. Comparative structure and histochemistry of silk-producing organs in arachnids. Pp. 160–186. *In* *Ecophysiology of Spiders*. (W Nentwig, ed.). Springer-Verlag, Berlin. doi: 10.1007/978-3-642-71552-5\_12
- Kovoor J. 1990. The silk-gland system in some Tetragnathinae (Araneae: Araneidae). Comparative anatomy and histochemistry. *Acta Zoologica Fennica* 190:215–221.
- Kovoor J, Lopez A. 1980. Variation de l'appareil séricigène dans la famille des Araneidae: Cas des genres *Cyclosa* Menge et *Nemoscolus* Simon. V<sup>ème</sup> Colloque d'Aracnologie d'Expression Française, Comptes-Rendus 119–127. [www.european-arachnology.org/esa/wp-content/uploads/2015/08/119-127\\_Kovoor.pdf](http://www.european-arachnology.org/esa/wp-content/uploads/2015/08/119-127_Kovoor.pdf)
- Kovoor J, Lopez A. 1982. Anatomie et histologie des glandes séricigènes des *Cyrtophora* (Araneae, Araneidae): affinités et corrélations avec la structure et la composition de la toile. *Revue Arachnologique* 4:1–21.
- Kovoor J, Lopez A. 1988. L'appareil séricigène des *Mecynogea* Simon (Araneae, Araneidae). *Revue Arachnologique* 7:205–212.
- Kovoor J, Peters HM. 1988. The spinning apparatus of *Polonecia producta* (Araneae, Uloboridae): Structure and histochemistry. *Zoomorphology* 108:47–59. doi: 10.1007/BF00312214
- Kovoor J, Zylberberg L. 1974. Ultrastructure des canaux des glandes aciniformes d'*Araneus diadematus* Clerck (Araneae, Argiopidae). *Annales des Sciences Naturelles, Zoologie et Biologie Animale, 12<sup>e</sup> Série* 16:5–25.
- Kulczyński W. 1909. Fragmenta Arachnologica, VIII. *Bulletin International de l'Académie des Sciences de Cracovie, Classe des Sciences Mathématiques et Naturelles* 1909:667–687.
- Lecigne S. 2011. Inventaire aranéologique dans la Province d'Izmir (Turquie) (Arachnida, Araneae). *Le Bulletin d'Arthropoda* 46:5–83.
- Le Peru B. 2011. *The Spiders of Europe, a Synthesis of Data: Volume 1, Atypidae to Theridiidae* (Mémoires de la Société Linnéenne de Lyon No. 2). SLL, Lyon.
- Leroy A, Leroy J. 2000. *Spiderwatch in Southern Africa*. Struik Publishers, Cape Town.
- Lin Y-J, Li S-Q. 2020. *Tibetima* gen. nov., a new genus of palpimanid spiders from Tibet, China (Araneae, Palpimanidae). *Acta Arachnologica Sinica* 29:85–88. doi: 10.3969/j.issn.1005-9628.2020.02.001
- Líznařová E, Sentenská L, Štáhlavský F, Pekár S. 2018. Stridulation can suppress cannibalism in a specialised araneophagous predator. *Behavioral Ecology and Sociobiology* 72:127. doi: 10.1007/s00265-018-2541-3
- Logunov DV, Gromov AV, Timokhanov VA. 2012. *Spiders of Kazakhstan*. Siri Scientific Press, Manchester.
- Lopez A, Juberthie-Jupeau L, Stowe MK. 1986. L'appareil séricigène de *Kaira alba* (Hentz) (Araneae: Araneidae). *Mémoires de la Société Royale Belge d'Entomologie* 33:119–128.
- Machado A de B. 1944. Observations inédites sur le colulus et les filières de quelques Aranéides, accompagnées de notes critiques sur la morphologie comparée des filières. *Arquivos do Museu Bocage* 15:13–52.
- Marusik YM, Guseinov EF. 2003. Spiders (Arachnida: Aranei) of Azerbaijan. 1. New family and genus records. *Arthropoda Selecta* 12:29–46. [kmkjournals.com/journals/AS/AS\\_Index\\_Volumes/AS\\_12/AS\\_12\\_1\\_029\\_046](http://kmkjournals.com/journals/AS/AS_Index_Volumes/AS_12/AS_12_1_029_046)
- Michálek O, Petráková L, Pekár S. 2017. Capture efficiency and trophic adaptations of a specialist and generalist predator: A comparison. *Ecology and Evolution* 7:2756–2766. doi: 10.1002/ece3.2812
- Michálek O, Kuhn-Nentwig L, Pekár S. 2019. High specific efficiency of venom of two prey-specialized spiders. *Toxins* 11:687. doi: 10.3390/toxins11120687
- Miller JA, Griswold CE, Scharff N, Řezáč M, Szűts T, Marhabaie M. 2012. The velvet spiders: an atlas of the Eresidae (Arachnida, Araneae). *ZooKeys* 195:1–144. doi: 10.3897/zookeys.195.2342
- Moon MJ, Kim WK. 1990. Ultrastructure of the aciniform glands in *Nephila clavata* L. Koch (Araneae: Araneidae). *Korean Arachnology* 5:195–206.
- Mullen GR. 1969. Morphology and histology of the silk glands in *Araneus sericatus* Cl. *Transactions of the American Microscopical Society* 88:232–240. doi: 10.2307/3224495
- Murphy JA, Roberts MJ. 2015. *Spider Families of the World and Their Spinnerets*. Part I: Text; Part II: Plates. British Arachnological Society, York.
- Oketch AD, Zonstein S, Kioko EN, Li S. 2020. Description of a new genus and three new species of the family Palpimanidae (Arachnida, Araneae) from Kenya. *African Invertebrates* 61:93–106. doi: 10.3897/AfrInvertebr.61.54004
- Park E-A, Moon M-J. 2009. Silk spinning apparatuses in the cribellate spider *Nurscia albofasciata* (Araneae: Titanoecidae). *Animal Cells and Systems* 13:153–160. doi: 10.1080/19768354.2009.9647207
- Pekár S, Líznařová E. 2023. Importance of spider prey for development of a specialized araneophagous predator (Araneae: Palpimanidae). *Journal of Arachnology* 51:114–117. doi: 10.1636/JoA-S-22-017
- Pekár S, Coddington JA, Blackledge TA. 2011a. Evolution of stenophagy in spiders (Araneae): evidence based on the comparative analysis of spider diets. *Evolution* 66:776–806. doi: 10.1111/j.1558-5646.2011.01471.x

- Pekár S, Šobotník J, Lubin Y. 2011b. Armoured spiderman: morphological and behavioural adaptations of a specialised araneophagous predator (Araneae: Palpimanidae). *Naturwissenschaften* 98:593–603. doi: 10.1007/s00114-011-0804-1
- Pekár S, García LF, Viera C. 2017. Trophic niches and trophic adaptations of prey-specialized spiders from the Neotropics: A guide. Pp. 247–274. In *Behaviour and Ecology of Spiders: Contributions from the Neotropical Region* (C Viera, MO Gonzaga, eds.). Springer, Cham. doi: 10.1007/978-3-319-65717-2\_10
- Pekár S, Líznavá E, Bočánek O, Zdráhal Z. 2018. Venom of prey-specialized spiders is more toxic to their preferred prey: A result of prey-specific toxins. *Journal of Animal Ecology* 87:1639–1652. doi: 10.1111/1365-2656.12900
- Pekár S, García LF, Bulbert MW. 2020. Spiders mimic the acoustic signalling of mutillid wasps to avoid predation: startle signalling or Batesian mimicry? *Animal Behaviour* 170:157–166. doi: 10.1016/j.anbehav.2020.10.015
- Pekár S, Petráková Dušátková L, Macháčková T, Slabý O, García LF, Haddad CR. 2022. Gut-content analysis in four species, combined with comparative analysis of trophic traits, suggests an araneophagous habit for the entire family Palpimanidae (Araneae). *Organisms Diversity & Evolution* 22:265–274. doi: 10.1007/s13127-021-00525-9
- Penney D. 2009. *Common Spiders & Other Arachnids of The Gambia, West Africa*. Siri Scientific Press, Manchester.
- Peters HM. 1983. Struktur und Herstellung der Fangfäden cribellater Spinnen (Arachnida: Araneae). *Verhandlungen des Naturwissenschaftlichen Vereins in Hamburg* (NF) 26:241–253.
- Peters HM. 1987. Fine structure and function of capture threads. Pp. 187–202. In *Ecophysiology of Spiders*. (W Nentwig, ed.). Springer-Verlag, Berlin. doi: 10.1007/978-3-642-71552-5\_13
- Peters HM. 1992. On the spinning apparatus and the structure of the capture threads of *Deinopis subrufus* (Araneae, Deinopidae). *Zoomorphology* 112:27–37. doi: 10.1007/BF01632992
- Peters HM, Kovoov J. 1989. Die Herstellung der Eierkokons bei der Spinne *Polonecia producta* (Simon, 1873) in Beziehung zu den Leistungen des Spinnapparates [The construction of egg-cases by the spider *Polonecia producta* (Simon, 1873) in relation to the functions of the spinning apparatus]. *Zoologische Jahrbücher: Abteilung für allgemeine Zoologie und Physiologie der Tiere* 93:125–144.
- Petrunkevitch A. 1933. An inquiry into the natural classification of spiders, based on a study of their internal anatomy. *Transactions of the Connecticut Academy of Arts and Sciences* 31:299–389, Plates I–XIII, Tables I–II.
- Petrunkevitch A. 1942. A study of amber spiders. *Transactions of the Connecticut Academy of Arts and Sciences* 34:119–464, Plates I–LXIX.
- Platnick NI. 1975. A revision of the palpimanid spiders of the new subfamily Otiiothopinae (Araneae, Palpimanidae). *American Museum Novitates* 2562:1–32. hdl.handle.net/2246/2755
- Platnick NI. 1981. A review of the spider subfamily Palpimaninae (Araneae, Palpimanidae), I. *Bulletin of the British Arachnological Society* 5:169–173. www.britishtspiders.org.uk/system/files/library/050405.pdf
- Platnick NI (ed.). 2020. *Spiders of the World, a Natural History*. Princeton University Press, Princeton.
- Platnick NI, Coddington JA, Forster RR, Griswold CE. 1991. Spinneret morphology and the phylogeny of haplogyne spiders (Araneae, Araneomorphae). *American Museum Novitates* 3016:1–73. hdl.handle.net/2246/5043
- Platnick NI, Griswold CJ, Ramírez MJ. 1999. On the genera of the spider subfamily Otiiothopinae (Araneae, Palpimanidae). *American Museum Novitates* 3257:1–25. hdl.handle.net/2246/3099
- Pompozzi G, García LF, Petráková L, Pekár S. 2019. Distinct feeding strategies of generalist and specialist spiders. *Ecological Entomology* 44:129–139. doi: 10.1111/een.12683
- Prajapati DA, Hun NK, Raval JV. 2021. A new species and a new combination in *Palpimanus* Dufour, 1820 from India (Aranei: Palpimanidae). *Arthropoda Selecta* 30:541–545. doi: 10.15298/arthsel.30.4.09
- Ramírez MJ. 2014. The morphology and phylogeny of dionychan spiders (Araneae: Araneomorphae). *Bulletin of the American Museum of Natural History* 390:1–374. doi: 10.1206/821.1
- Ramírez MJ, Griswold CJ, Labarque FM, Izquierdo MA, Ledford JM, Miller JA, et al. 2014. The morphology and relationships of the walking mud spiders of the genus *Cryptothele* (Araneae: Zodariidae). *Zoologischer Anzeiger* 253:382–393. doi: 10.1016/j.jcz.2014.03.002
- Režáč M, Krejčí T, Goodacre SL, Haddad CR, Řezáčová V. 2017. Morphological and functional diversity of minor ampullate glands in spiders from the superfamily Amaurobioidea (Entelegynae: RTA clade). *Journal of Arachnology* 45:198–208. doi: 10.1636/JoA-16-010-Rezak.1
- Russell-Smith A, Allison R, Askins M, Blumsom W, Snazell R, Spilling C. 2011. A provisional checklist and gazetteer of the spiders of Chios, Greece (Arachnida: Araneae). *Bulletin of the British Arachnological Society* 15:133–167. www.britishtspiders.org.uk/system/files/library/150501.pdf
- Scharff N, Coddington JA. 1997. A phylogenetic analysis of the orb-weaving spider family Araneidae (Arachnida, Araneae). *Zoological Journal of the Linnean Society* 120:355–434. doi: 10.1111/j.1096-3642.1997.tb01281.x
- Schniepp HC, Koebley SR, Vollrath F. 2013. Brown recluse spider's nanometer scale ribbons of stiff extensible silk. *Advanced Materials* 25:7028–7032. doi: 10.1002/adma.201302740
- Simon E. 1892–1893. *Histoire Naturelle des Araignées, 2<sup>e</sup> Édition, Volume 1*, Pp. 1–488. Librairie Encyclopédique de Roret, Paris.
- Sonavane S, Westermark P, Rising A, Holm L. 2023. Regionalization of cell types in silk glands of *Larinioides sclopetarius* suggest that spider silk fibers are complex layered structures. *Scientific Reports* 13:22273. doi: 10.1038/s41598-023-49587-z
- Tillinghast EK, Townley MA. 1994. Silk glands of araneid spiders: selected morphological and physiological aspects. Pp. 29–44. In *Silk Polymers: Materials Science and Biotechnology* (ACS Symposium Series 544). (D Kaplan, WW Adams, B Farmer, C Viney, eds.). American Chemical Society, Washington, DC. doi: 10.1021/bk-1994-0544.ch003
- Townley MA, Harms D. 2017. Comparative study of spinning field development in two species of araneophagic spiders (Araneae, Mimetidae, *Australomimetus*). *Evolutionary Systematics* 1:47–75. doi: 10.3897/evolsyst.1.14765
- Townley MA, Harms D. 2020. Hers and his: Silk glands used in egg sac construction by female spiders potentially repurposed by a ‘modern’ male spider. *Scientific Reports* 10:6663. doi: 10.1038/s41598-020-63521-7
- Townley MA, Tillinghast EK. 2003. On the use of ampullate gland silks by wolf spiders (Araneae, Lycosidae) for attaching the egg sac to the spinnerets and a proposal for defining nubbins and tartipores. *Journal of Arachnology* 31:209–245. doi: 10.1636/0161-8202(2003)031[0209:OTUOAG]2.0.CO;2
- Townley MA, Tillinghast EK. 2009. Developmental changes in spider spinning fields: a comparison between *Mimetus* and *Araneus* (Araneae: Mimetidae, Araneidae). *Biological Journal of the Linnean Society* 98:343–383. doi: 10.1111/j.1095-8312.2009.01297.x
- Townley MA, Tillinghast EK. 2013. Aggregate silk gland secretions of araneoid spiders. Pp. 283–302. In *Spider Ecophysiology*. (W Nentwig, ed.). Springer-Verlag, Heidelberg. doi: 10.1007/978-3-642-33989-9\_21
- Townley MA, Horner NV, Cherim NA, Tugmon CR, Tillinghast EK. 1991. Selected aspects of spinning apparatus development in *Araneus cavaticus* (Araneae, Araneidae). *Journal of Morphology* 208:175–191. doi: 10.1002/jmor.1052080204
- Townley MA, Tillinghast EK, Cherim NA. 1993. Moulting-related changes in ampullate silk gland morphology and usage in the araneid spider *Araneus cavaticus*. *Philosophical Transactions of the Royal Society of London, Series B* 340:25–38. doi: 10.1098/rstb.1993.0046
- Townley MA, Harms D, Benjamin SP. 2013. Phylogenetic affinities of *Phobetinus* to other pirate spider genera (Araneae: Mimetidae) as indicated by spinning field morphology. *Arthropod Structure & Development* 42:407–423. doi: 10.1016/j.asd.2013.04.003
- Tutar O, Yağmur EA. 2023. Spider (Araneae) fauna of İzmir Peninsula (Çeşme, Karaburun, Urla), Türkiye. *Serket* 19:197–222.
- Uhl G, Elias DO. 2011. Communication. Pp. 127–189. In *Spider Behaviour: Flexibility and Versatility* (ME Herberstein, ed.). Cambridge University Press, Cambridge. doi: 10.1017/CBO9780511974496.006



- Uhl G, Schmitt M. 1996. Stridulation in *Palpimanus gibbulus* Dufour (Araneae:Palpimanidae). *Revue Suisse de Zoologie* volume hors série II: 649–660. [www.biodiversitylibrary.org/page/43628782#page/283/mode/1up](http://www.biodiversitylibrary.org/page/43628782#page/283/mode/1up)
- Wąsowska S. 1969. Particularités de l'appareil séricigène des mâles *Clubiona phragmitis* C. L. Koch. *Zoologica Poloniae* 19:505–515.
- Watts P, Townley M. 2022. *Palpimanus* abdomen lifts.mov.figshare.Media. Online at [figshare.com/articles/media/Palpimanus\\_abdomen\\_lifts\\_mov/21222380](https://figshare.com/articles/media/Palpimanus_abdomen_lifts_mov/21222380). doi: 10.6084/m9.figshare.21222380.v1
- Wheeler WC, Coddington JA, Crowley LM, Dimitrov D, Goloboff PA, Griswold CE. et al. 2017. The spider tree of life: phylogeny of Araneae based on target-gene analyses from an extensive taxon sampling. *Cladistics* 33:574–616. doi: 10.1111/cla.12182
- Wiśniewski H. 1986. Studies on the spinning apparatus of *Clubiona phragmitis* C. L. Koch (Araneida, Clubionidae). II. The structure of the internal spinning apparatus. *Zoologica Poloniae* 33:83–104, Plates I–V.
- Wolff JO, Michalik P, Ravelo AM, Herberstein ME, Ramírez MJ. 2021. Evolution of silk anchor structure as the joint effect of spinning behavior and spinneret morphology. *Integrative and Comparative Biology* 61:1411–1431. doi: 10.1093/icb/icab003
- World Spider Catalog. 2024. World Spider Catalog, Version 25.0 Natural History Museum, Bern. Online at [wsc.nmbe.ch](http://wsc.nmbe.ch), accessed on 11 March 2024. doi: 10.24436/2
- World Weather Online. 2022. Chios Climate Weather Averages. Online at [www.worldweatheronline.com/chios-weather-averages/north-aegean/gr.aspx](http://www.worldweatheronline.com/chios-weather-averages/north-aegean/gr.aspx), accessed on 25 September 2022.
- Yu L, Coddington JA. 1990. Ontogenetic changes in the spinning fields of *Nuctenea cornuta* and *Neoscona theisi* (Araneae, Araneidae). *Journal of Arachnology* 18:331–345. [www.jstor.org/stable/3705439](http://www.jstor.org/stable/3705439)
- Zamani A, Marusik YM. 2021. A new genus and ten new species of spiders (Arachnida, Araneae) from Iran. *ZooKeys* 1054:95–126. doi: 10.3897/zookeys.1054.70408
- Zonstein S, Marusik YM. 2013. On *Levymanus*, a remarkable new spider genus from Israel, with notes on the Chediminae (Araneae, Palpimanidae). *ZooKeys* 326:27–45. doi: 10.3897/zookeys.326.5344
- Zonstein SL, Marusik YM. 2017. Descriptions of the two-eyed African spider genera *Chedimanops* gen. n. and *Hybosidella* gen. n. (Araneae, Palpimanidae, Chediminae). *African Invertebrates* 58:23–47. doi: 10.3897/AfrInvertebr.57.11448
- Zonstein SL, Marusik YM. 2019. On the revisited types of four poorly known African species of *Palpimanus* (Araneae, Palpimanidae). *African Invertebrates* 60:83–95. doi: 10.3897/AfrInvertebr.52.34229
- Zonstein SL, Marusik YM. 2020. Two new species of *Diaphorocellus* Simon, 1893 from Madagascar (Araneae, Palpimanidae). *African Invertebrates* 61:1–15. doi: 10.3897/AfrInvertebr.61.47048
- Zonstein S, Marusik YM. 2022. Descriptions of *Sceliraptor* gen. n. and two new species from Kenya (Araneae, Palpimanidae). *Arachnology* 19(Special Issue):257–264. [www.britishtspiders.org.uk/system/files/library/190018.pdf](http://www.britishtspiders.org.uk/system/files/library/190018.pdf)

*Manuscript received 1 October 2022, revised 5 January 2023, accepted 6 January 2023.*